Electronic Supplementary Material (ESI) for Photochemical & Photobiological Sciences.

Kinetic Analysis of Tautomer Forms of Aromatic-Urea Compounds with Acetate Ions: Solvent Effect of Excited State Intermolecular Proton Transfer

Hisato Matsumoto, Satomi Ikedu, Takeyuki Tosaka, Yoshinobu Nishimura and Tatsuo Arai[a]

Graduate School of Pure and Applied Sciences, University of Tsukuba,

1-1-1 Tennoudai, Tsukuba, Ibaraki 305-8571 Japan.

E-mail: arai@chem.tsukuba.ac.jp

Contents

Experimental

Methods

^{1}H NMR spectra were recorded on a Bruker ARX-400 (400 MHz for ^{1}H NMR) spectrometer using DMSO-d_6 as a solvent and tetramethylsilane as an internal standard. Absorption and fluorescence spectra were measured on Shimadzu UV-1600 and Hitachi F–4500 fluorescence spectrometers, respectively. Fluorescence decay measurements were performed using a time-correlated single-photon counting method. Laser excitation at 375 nm was performed using a diode laser (PicoQuant, LDH-P-C-375) with a power control unit (PicoQuant, PDL 800-B), with a repetition rate of 2.5 MHz. The temporal profiles of the fluorescence decay were detected by a microchannel plate photomultiplier (Hamamatsu, R3809U) equipped with a TCSPC computer board module (Becker and Hickl, SPC630). The full width at half-maximum (fwhm) value of the instrument response function was 51 ps.[1] The values of χ^2 and the Durbin–Watson parameters were used to determine the quality of the fit obtained by nonlinear regression.[2] DMSO, MeCN, THF, toluene, (spectroscopic grade, Wako Pure Chemical Industries, Japan) and were used as a solvent without further purification. Acetate ions were in the form of tetrabutylammonium acetate (TBAAc), which contains a tetrabutylammonium cation (Sigma-Aldrich, Japan). All measurements were carried out at room temperature under an Ar atmosphere. The concentrations were adjusted so that the absorption maximum of the excitation wavelength was about 0.1 for each sample.

Synthesis

All solvents and *tert*-dodecanethiol, 1-chloro-4-nitrobenzene, *m*-chloroperbenzoic acid, $SnCl_2 \cdot 2H_2O$, diphenylphosphoryl azide, triethylamine and 9,10-anthracenedicarboxylic acid were purchased from Wako Pure Chemical Industries Ltd., Japan, Tokyo Chemical Industry Co., Ltd., Japan or Aldrich, USA and were used without further purification. All compounds were synthesized as shown in Scheme S1.[3,4]

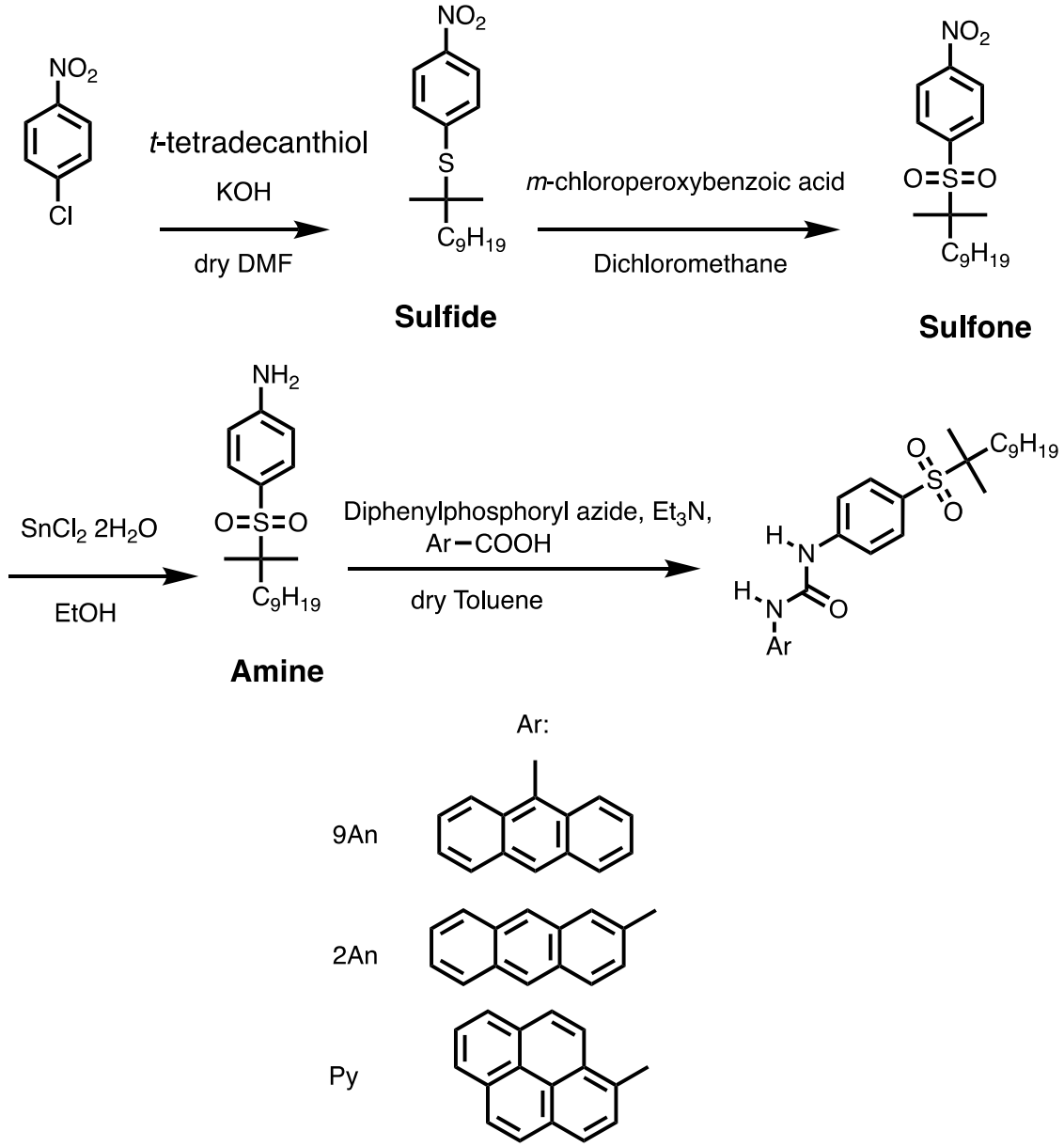

Scheme S1. Synthesis of **9An**, **2An** and **Py**.

Sulfide

tert-dodecanethiol (9.9 mL, 41.6 mmol) and KOH (3.01 g, 53.8 mmol) were added to a solution of 1-chloro-4-nitrobenzene (4.99 g, 31.7 mmol) in dry DMF (50 mL). The resulting reaction mixture was stirred at 100°C for 10 h and then the solvent was evaporated to dryness under reduced pressure. The solid residue was taken up with 2N HCl (50 mL) and CH_2Cl_2 (50 mL). The organic layer was separated, washed with water up to neutrality, dried with Na_2SO_4 and the solvent completely evaporated under reduced pressure. Purification of the oily residue by column chromatography (hexane/dichloromethane = 5:1) yielded red oily liquid (7.03 g, 69%). ^{1}H NMR ($CDCl_3$, 270 MHz): δ = 0.80-1.60 (m, 25H), 7.60-7.66 (m, 2H), 8.12-8.14 (m, 2H)

Sulfone

A solution of *m*-chloroperbenzoic acid (13.65 g, 51.4 mmol) in CH_2Cl_2 (100 mL) was added dropwise to a solution of **Sulfide** (6.56 g, 20.17 mmol) in CH_2Cl_2 (100 mL), maintained at 0°C through an external ice bath. The resulting reaction mixture was stirred at room temperature for 6 h, and then washed in turn with a saturated aqueous solution of Na_2CO_3 and with a saturated aqueous solution $NaHCO_3$. The separated organic layer was dried with Na_2SO_4 and the solvent was evaporated under reduced pressure to give red oily liquid (6.12 g, 86%). ^{1}H NMR ($CDCl_3$, 400 MHz): δ = 0.87-1.67 (m, 25H), 8.05-8.08 (m, 2H), 8.37-8.42 (m, 2H)

Amine

$SnCl_2 \cdot 2H_2O$ (19.67 g, 87.1 mmol) was added to a solution of **Sulfone** (6.12 g, 17.2 mmol) in ethanol (100 mL). The resulting heterogeneous solution was refluxed whilst stirring for 3 h and then the solvent was completely removed under reduced pressure. The residue was taken up with 1N aqueous solution of NaOH (90 mL) and extracted with chloroform. The separated organic phase was dried with Na_2SO_4 and the solvents evaporated to dryness under reduced pressure to give oily liquid (2.83 g, 51%). ^{1}H NMR ($CDCl_3$, 270 MHz): δ = 0.86-1.62 (m, 25H), 4.16 (s, 2H), 6.70-6.73 (d, J = 8.2 Hz, 2H), 7.61-7.63 (d, J = 8.2 Hz, 2H).

9An

To a two-neck round-bottom flask (100 mL) were added 9-anthracenecarboxylic acid (451 mg, 2.01 mmol), toluene (20 mL), triethylamine (324 µl, 2.45 mmol), and diphenylphosphoryl azide (585 µl, 2.34 mmol). After the mixture was stirred for 30 min at 80°C, **Amine** (543 mg, 1.67 mmol) in THF (10 mL) was added, and the mixture was refluxed for 4 h. The residue was completely evaporated under reduced pressure. Purification of the oily residue by column chromatography (ethyl acetate: hexane = 1:3), gave light yellow solid (376 mg, 41%). ^{1}H NMR (DMSO-d_6, 400 MHz): δ 0.85-1.58 (m, 25H), 7.52-7.60 (m, 4H), 7.67-7.77 (m, 4H), 8.12-8.20 (m, 4H), 8.61 (s, 1H), 8.96 (s, 1H), 9. 07 (s, 1H), δ 9.40 (s, 1H). ^{13}C NMR (DMSO-d_6, 400 MHz): δ 8.78, 12.48, 14.40, 14.72, 15.05, 20.79, 22.90, 29.67, 62.52, 65.40, 66.24, 117.8, 124.2, 126.0, 126.2, 126.5, 128.0, 128.9, 129.2, 129.6, 131.6, 131.8, 145.8, 154.4. Anal. Calcd. for $C_{33}H_{40}N_2O_3S$: C, 72.76; H, 7.40; N, 5.14. Found: C, 72.89; H, 7.47; N, 5.11.

2An

To a two-neck round-bottom flask (100 mL) were added 2-anthracenecarboxylic acid (403 mg, 1.81 mmol), toluene (15 mL), triethylamine (215 μL, 1.55 mmol), and diphenylphosphoryl azide (525 μL, 2.10 mmol). After the mixture was stirred for 30 min at 80°C, **Amine** (503 mg, 1.54 mmol) in THF (10 mL) was added, and the mixture was refluxed for 4 h. The residue was completely evaporated under reduced pressure. Purification of the oily residue by column chromatography (ethyl acetate: hexane = 2:3), gave light yellow solid (167 mg, 20%). ^{1}H NMR (DMSO-d_6, 400 MHz): δ 0.80-1.60 (m, 25H), 7.43-7.52 (m, 3H), 7.75-7.79 (m, 4H), 8.02-8.07 (m, 3H), 8.31 (s, 1H), 8.44 (s, 1H), 8.50, (s, 1H), 9.17 (s, 1H), δ 9.40 (s, 1H). ^{13}C NMR (DMSO-d_6, 400 MHz): δ 7.25, 8.79, 11.10, 14.36, 14.67, 18.91, 19.59, 20.87, 27.58, 46.08, 57.63, 112.9, 117.9, 121.4, 122.5, 125.1, 125.3, 126.1, 126.4, 128.1, 128.6, 128.7, 129.5, 130.7, 131.6, 132.2, 132.3, 136.7, 145.0, 152.7. Anal. Calcd. for $C_{33}H_{40}N_2O_3S$: C, 72.76; H, 7.40; N, 5.14. Found: C, 72.69; H, 7.35; N, 5.42.

Py

To a two-neck round-bottom flask (50 mL) were added 1-pyrenecarboxylic acid (297 mg, 1.21 mmol), toluene (15 mL), triethylamine (180 μl, 1.30 mmol), and diphenylphosphoryl azide (270 μl, 1.26 mmol). After the mixture was stirred for 30 min at 80°C, **Amine** (356 mg, 1.10 mmol) in THF (10 mL) was added, and the mixture was refluxed for 3 h. The residue was completely evaporated under reduced pressure. Purification of the oily residue by column chromatography (ethyl acetate: hexane = 1:1), gave light yellow solid (376 mg, 41%). ^{1}H NMR (DMSO-d_6, 400 MHz): δ 0.70-1.59 (m, 25H), 7.78 (d, J = 7.4 Hz, 4H), 8.40-8.42 (m, 3H), 8.27-8.37 (m, 5H), 8.56 (s, 1H), 9.38 (s, 1H), δ 9.72 (s, 1H). ^{13}C NMR (DMSO-d_6, 400 MHz): δ 10.61, 12.53, 18.57, 23.16, 23.37, 26.69, 29.76, 35.01, 37.83, 51.71, 59.95, 117.5, 117.8, 119.4, 121.1, 122.3, 124.5, 124.6, 125.0, 125.2, 125.6, 125.8, 126.4, 126.9, 127.6, 127.8, 128.0, 131.1, 131.5, 132.8, 153.3. Anal. Calcd. for $C_{35}H_{40}N_2O_3S$: C, 73.91; H, 7.09; N, 4.93; O, 8.44; S, 5.64. Found: C, 73.90; H, 6.88; N, 4.86.

9,10An was synthesized by past synthesis methods.[5]

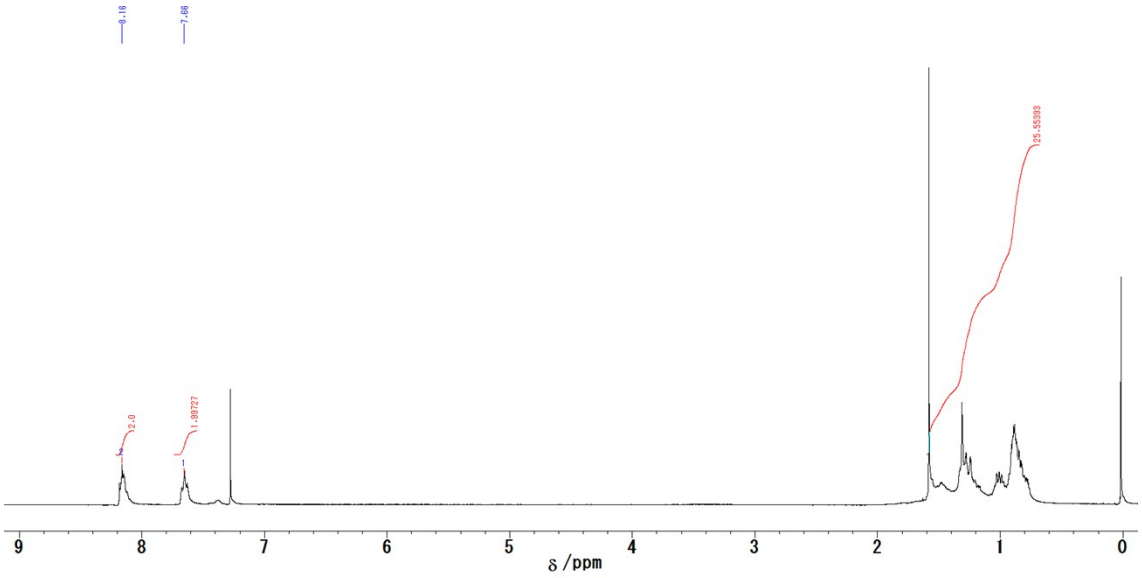

Fig. S1. ^{1}H NMR spectrum of **Sulfide** in $CDCl_3$ at 298 K.

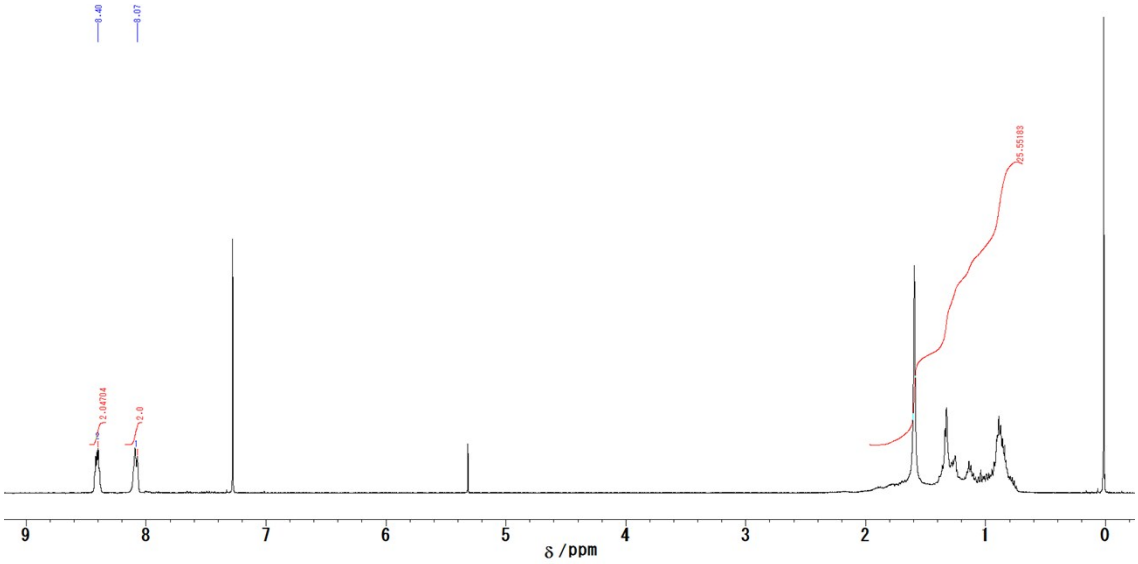

Fig. S2. ^{1}H NMR spectrum of **Sulfone** in $CDCl_3$ at 298 K.

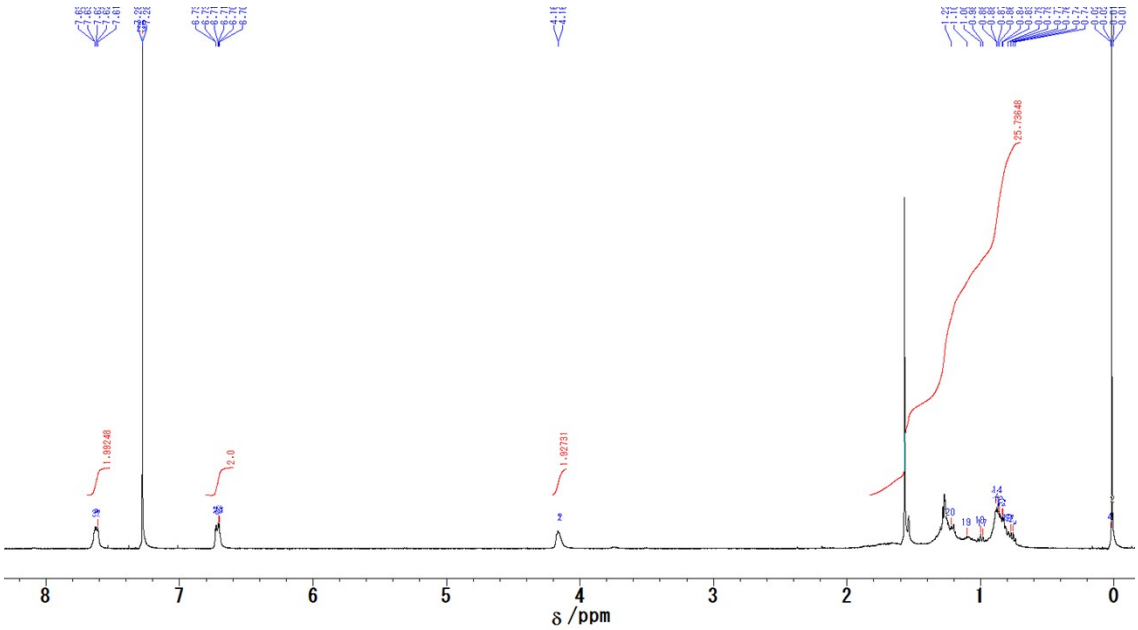

Fig. S3. ^{1}H NMR spectrum of **Amine** in $CDCl_3$ at 298 K.

(a)

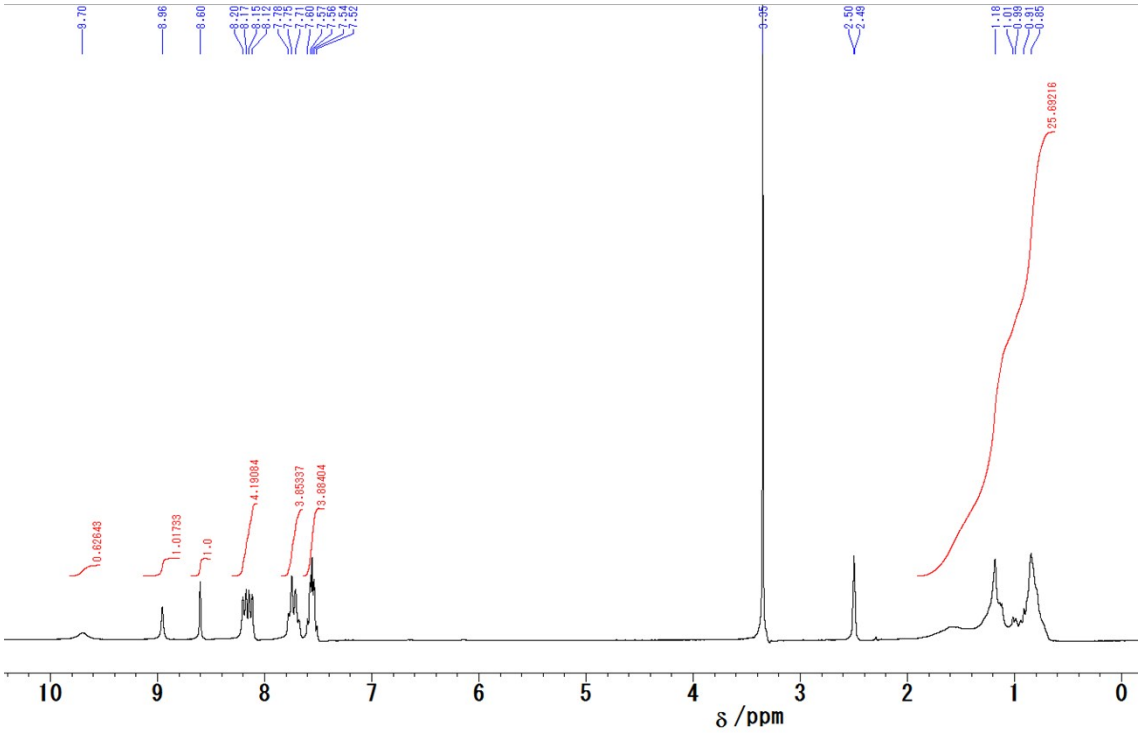

(b)

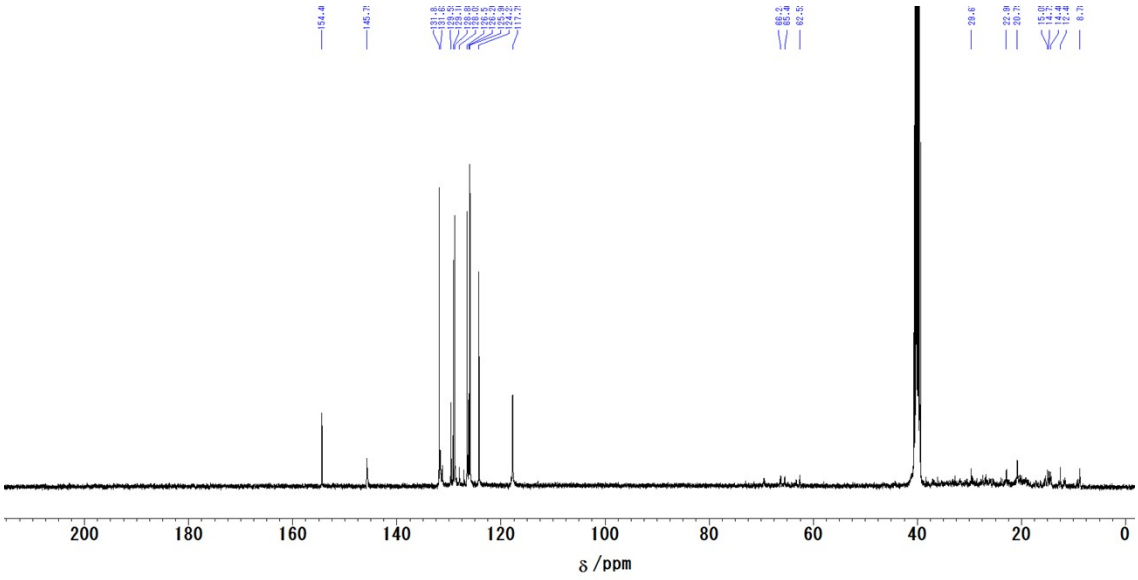

Fig. S4. (a) ^{1}H NMR spectrum of **9An** in DMSO-d_6 at 298 K. (b) ^{13}C NMR spectrum of **9An** in DMSO-d_6 at 298 K.

(a)

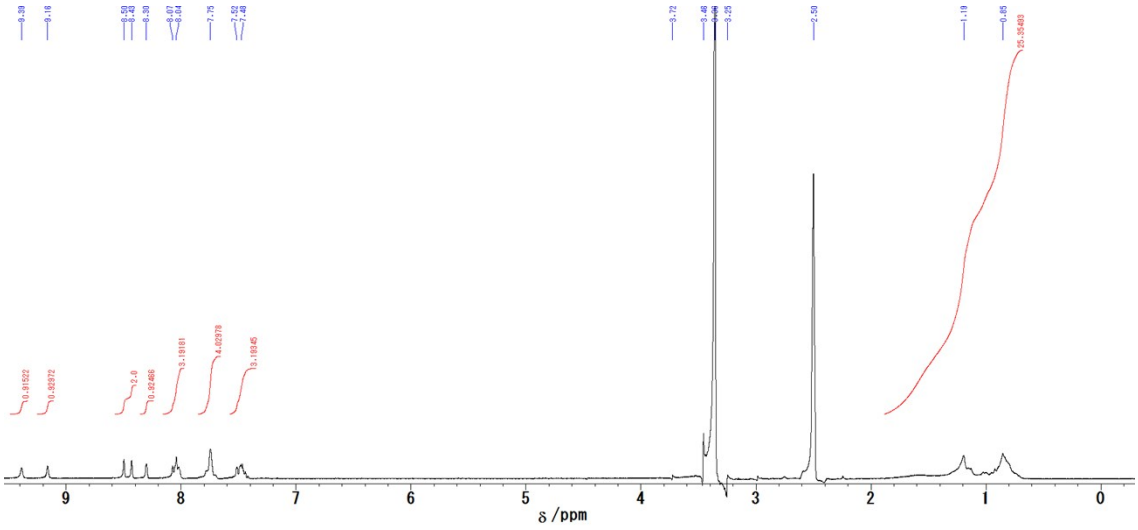

(b)

Fig. S5. (a) ^{1}H NMR spectrum of **2An** in DMSO-d_6 at 298 K. (b) ^{13}C NMR spectrum of **2An** in DMSO-d_6 at 298 K.

(a)

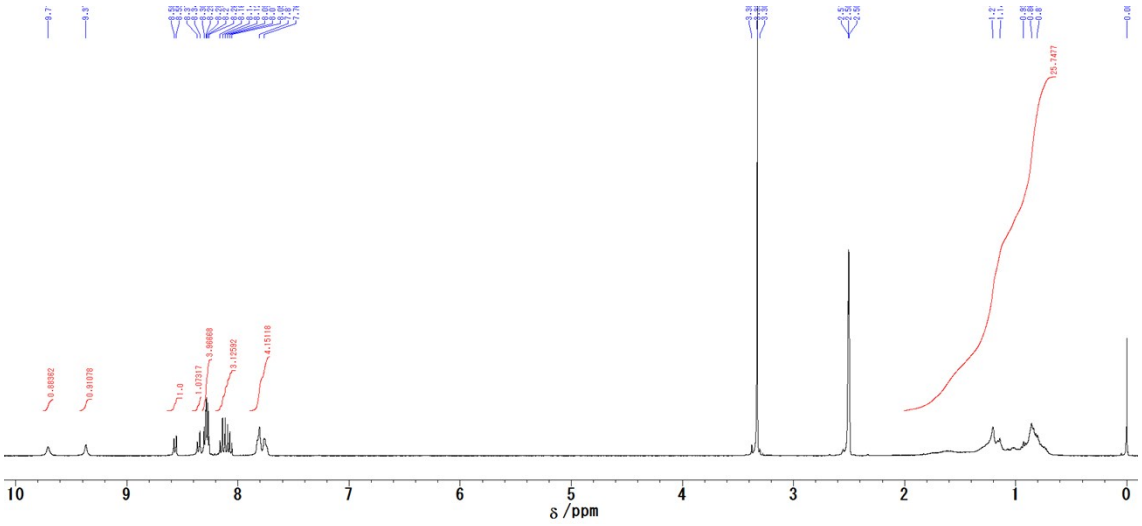

(b)

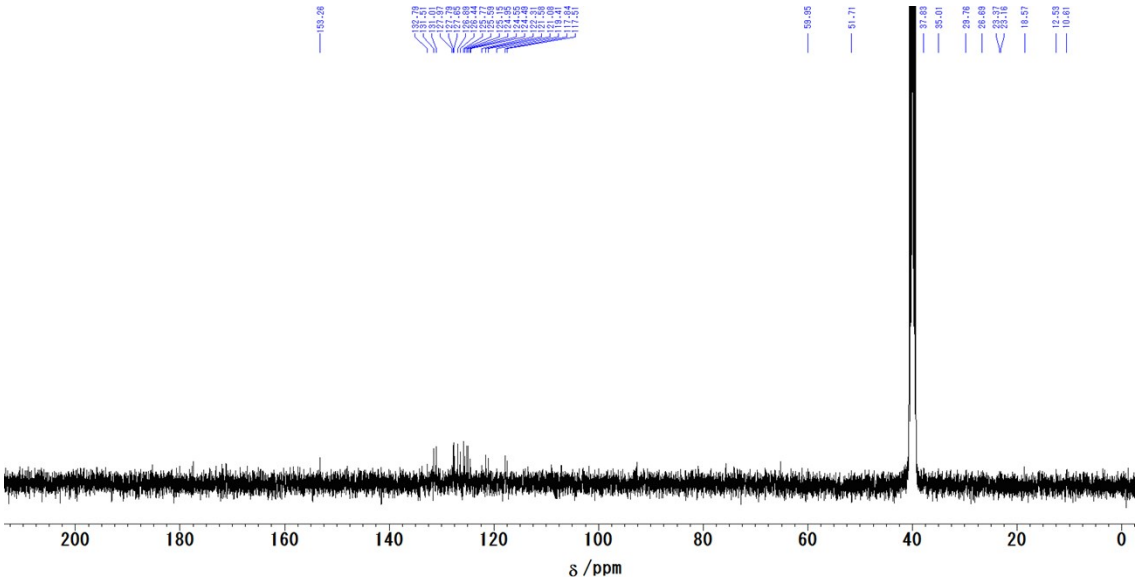

Fig. S6. (a) ^{1}H NMR spectrum of **Py** in DMSO-d_6 at 298 K. (b) ^{13}C NMR spectrum of **Py** in DMSO-d_6 at 298 K.

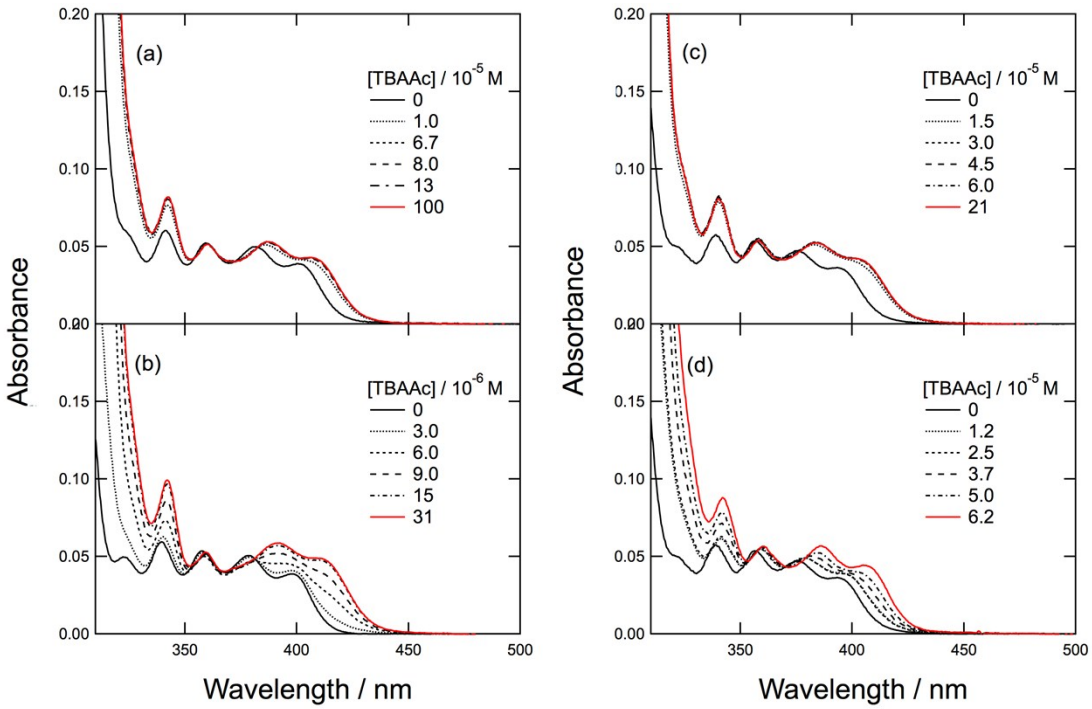

Fig. S7. Changes in the absorption spectra of **2An** in (a) DMSO (1.0×10^{-5} M), (b) THF (1.1×10^{-5} M), (c) MeCN (1.0×10^{-5} M) and (d) toluene (1.1×10^{-5} M) by the addition of TBAAc.

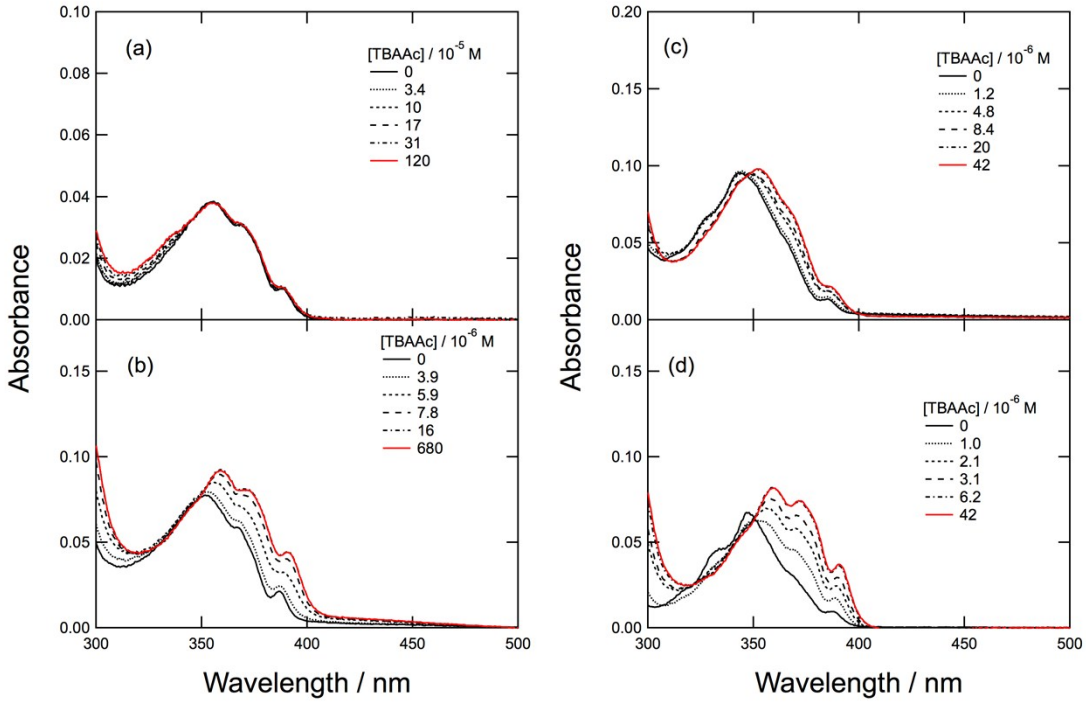

Fig. S8. Changes in the absorption spectra of **Py** in (a) DMSO (1.1×10^{-6} M), (b) THF (2.2×10^{-6} M), (c) MeCN (2.9×10^{-6} M) and (d) toluene (1.9×10^{-6} M) by the addition of TBAAc.

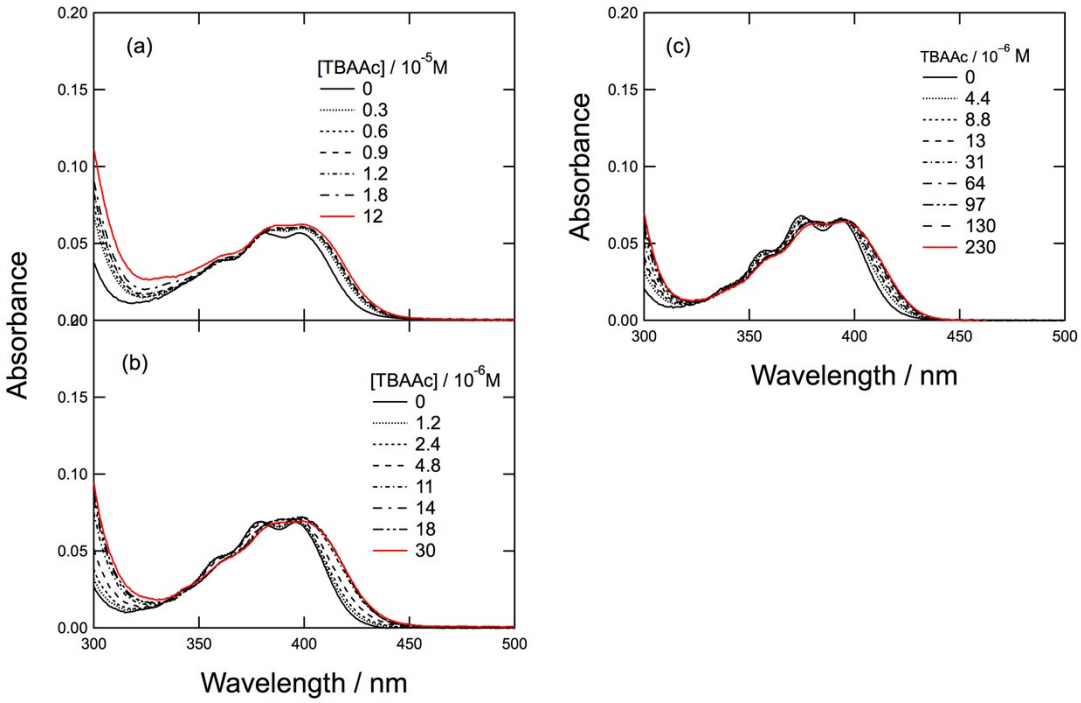

Fig. S9. Changes in the absorption spectra of **9,10An** in (a) DMSO (6.2×10^{-6} M), (b) THF (7.1×10^{-6} M) and (c) MeCN (7.4×10^{-6} M) by the addition of TBAAc.

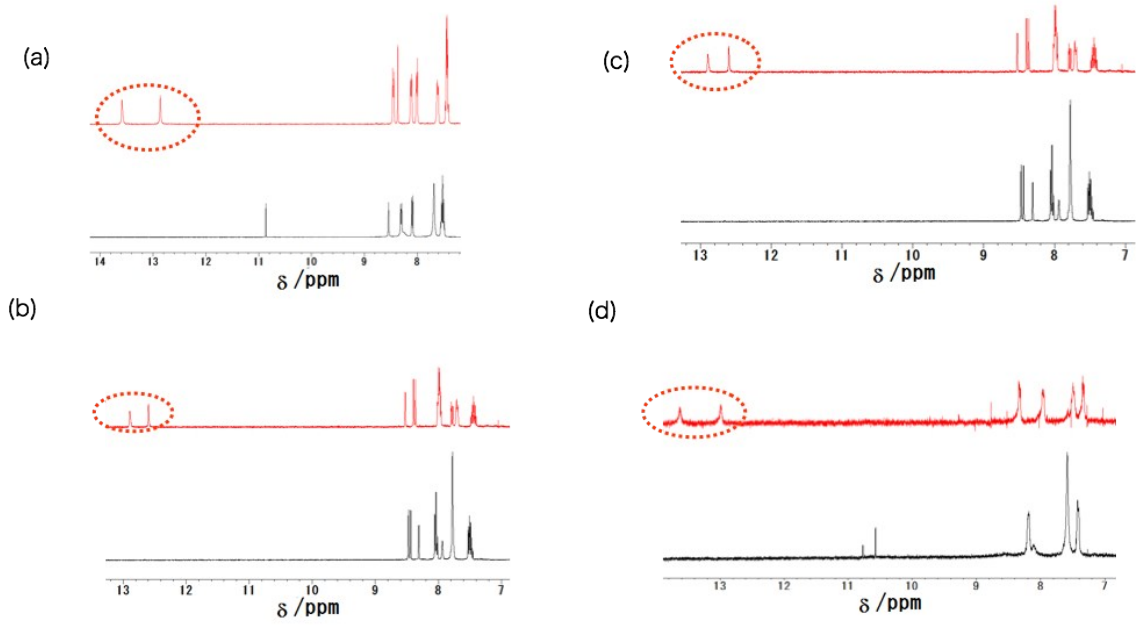

Fig. S10 ^{1}H NMR spectra of (a) **9An**, (b) **2An**, (c) **Py** and (d) **9,10An** in the presence (top) and absence (bottom) of TBAAc in THF-d_8.

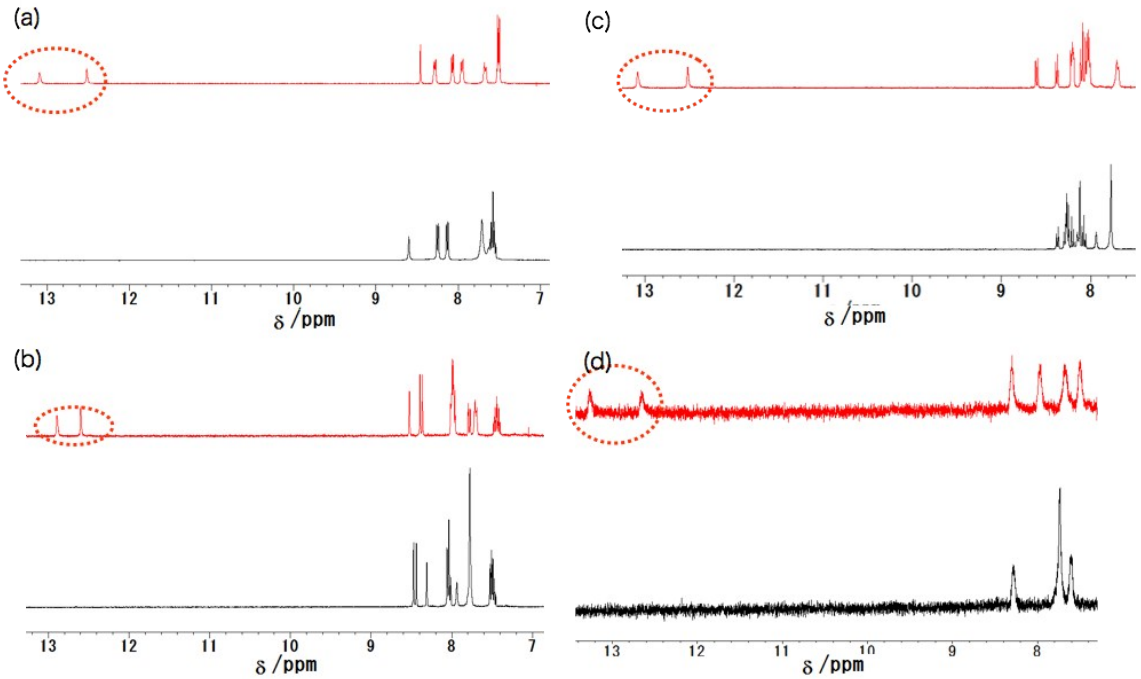

Fig. S11 ^{1}H NMR spectra of (a) **9An**, (b) **2An**, (c) **Py** and (d) **9,10An** in the presence (top) and absence (bottom) of TBAAc in MeCN-d_3.

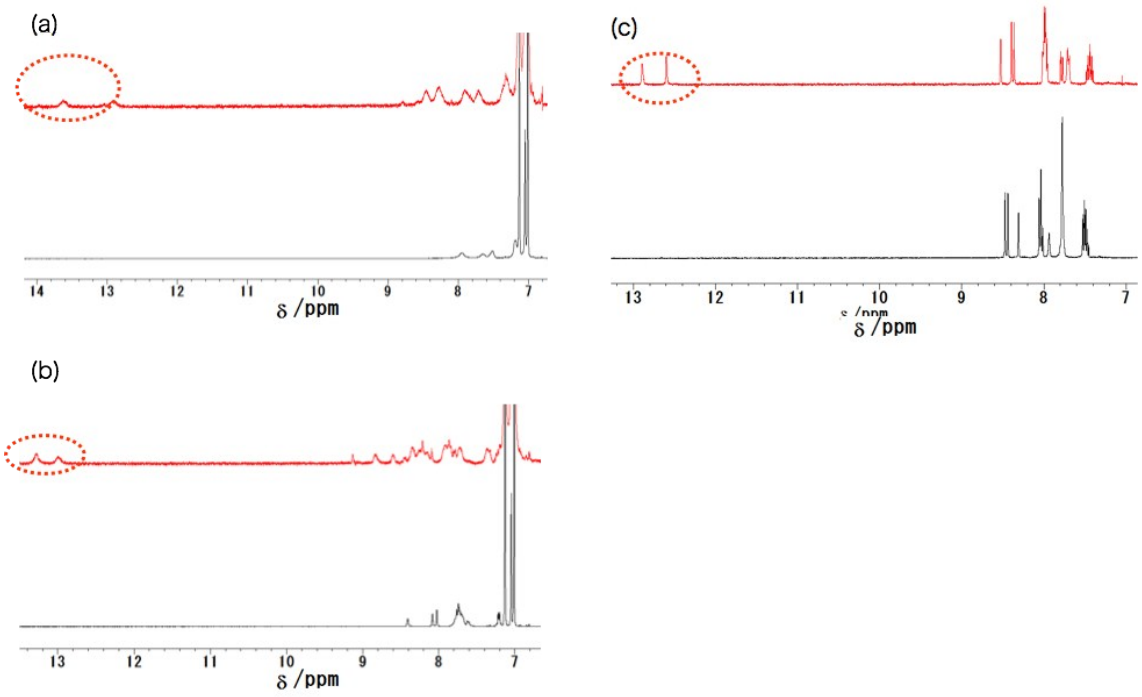

Fig. S12. ^{1}H NMR spectra of (a) **9An**, (b) **2An** and(c) **Py** in the presence (top) and absence (bottom) of TBAAc in toluene-d_8.

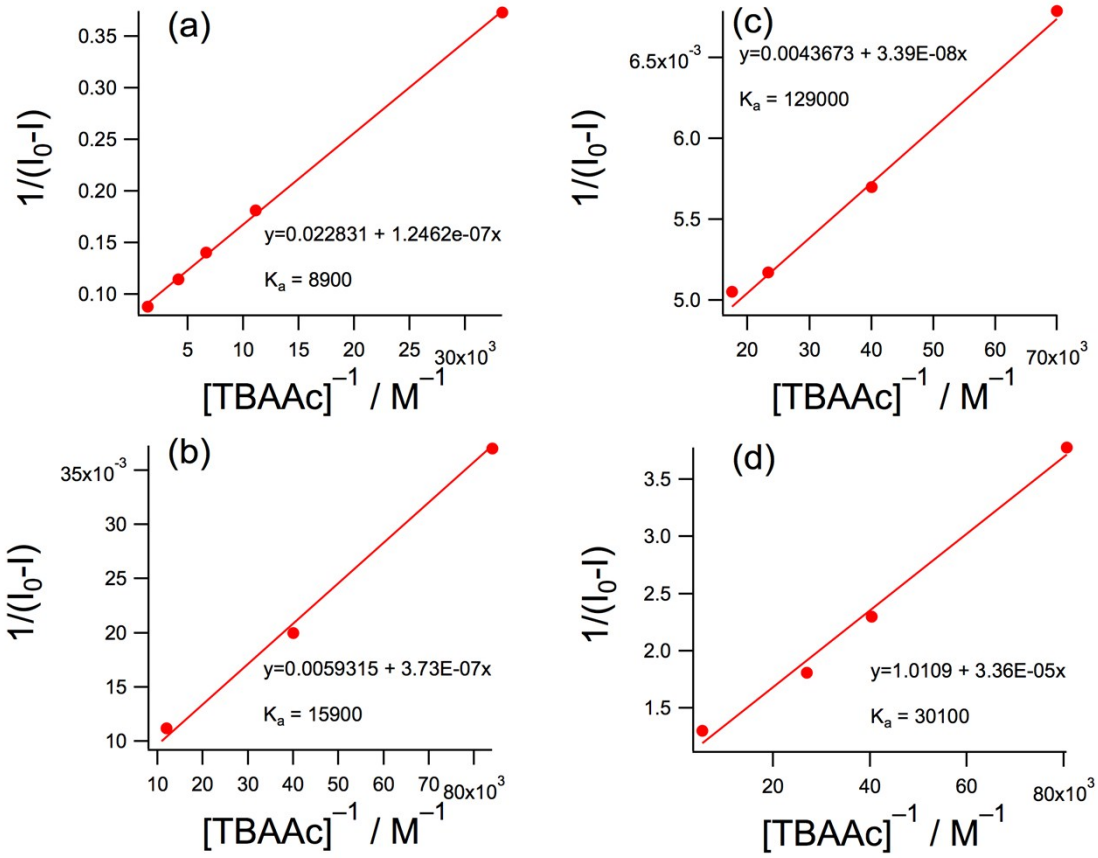

Fig. S13. Theoretical fits to estimate association constants of **9An** in (a) DMSO, (b) THF, (c) MeCN and (d) toluene.

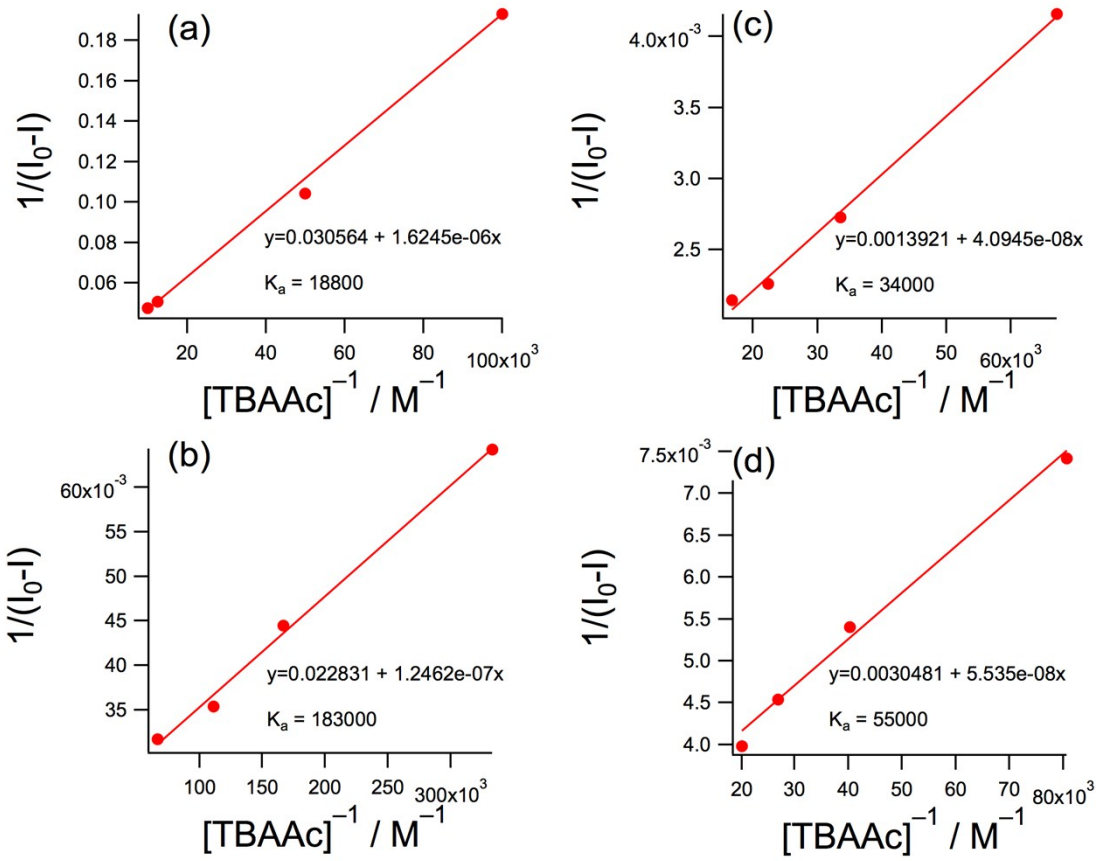

Fig. S14. Theoretical fits to estimate association constants of **2An** in (a) DMSO, (b) THF, (c) MeCN and (d) toluene.

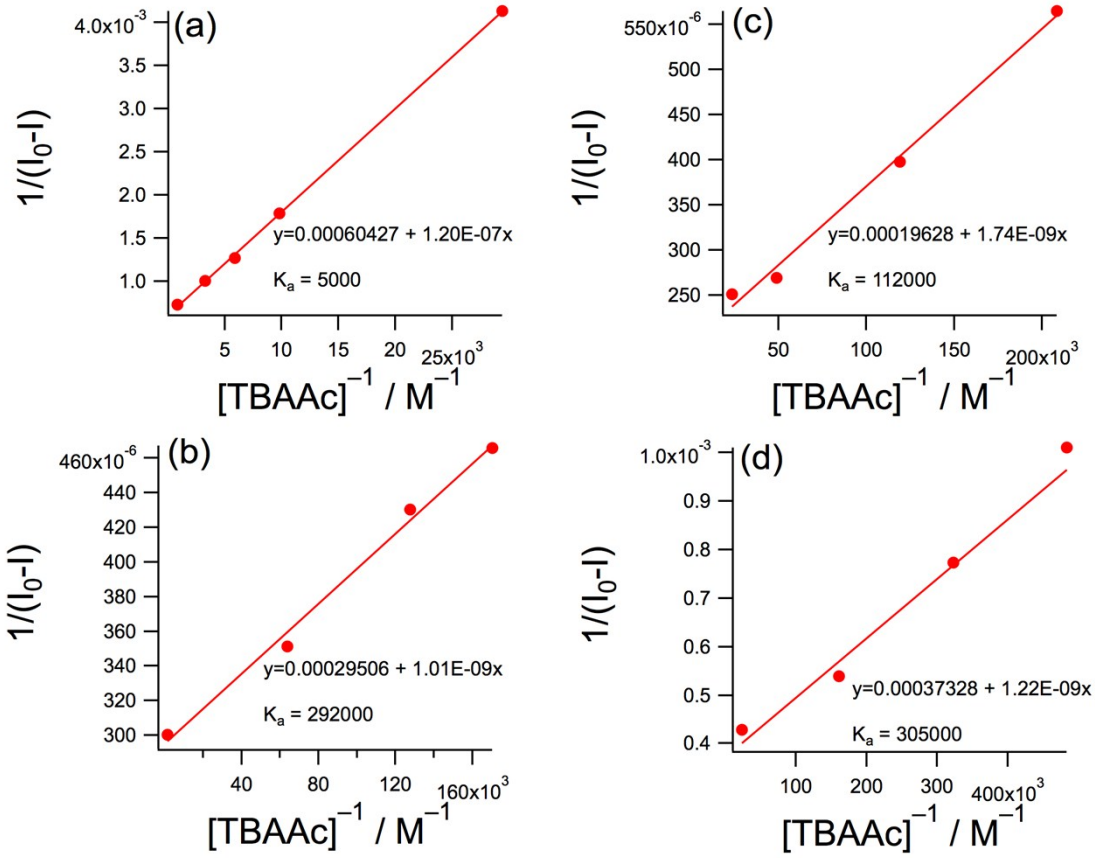

Fig. S15. Theoretical fits to estimate association constants of **Py** in (a) DMSO, (b) THF, (c) MeCN and (d) toluene.

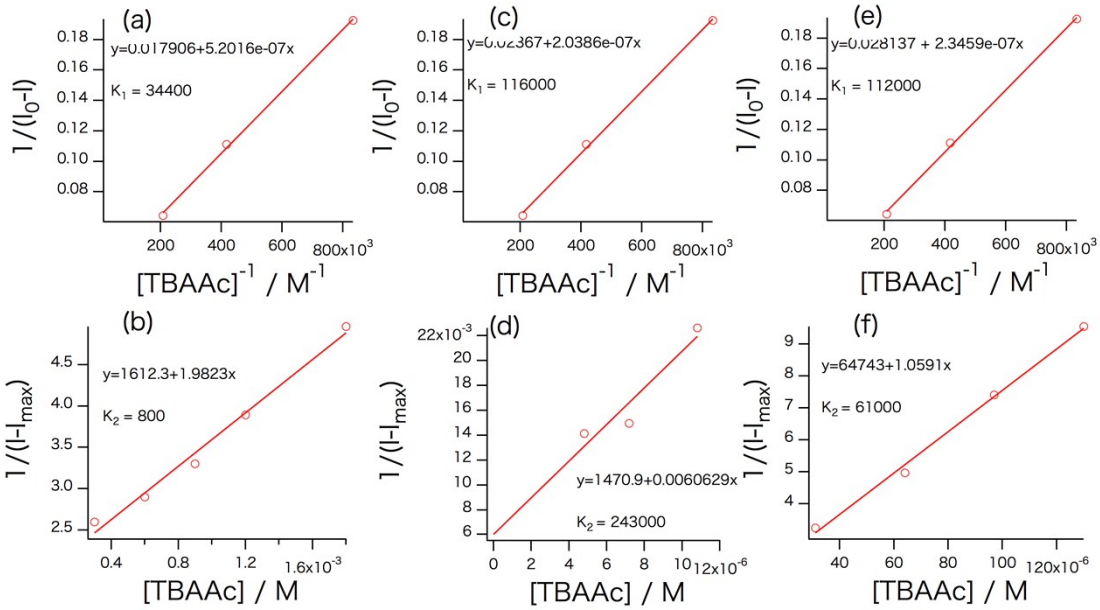

Fig. S16. Theoretical fits to estimate association constants of **9,10An** in (a) DMSO (K_{a1}), (b) DMSO (K_{a2}), (c) THF (K_{a1}), (d) THF (K_{a2}), (e) MeCN (K_{a1}), and (f) MeCN (K_{a2}).

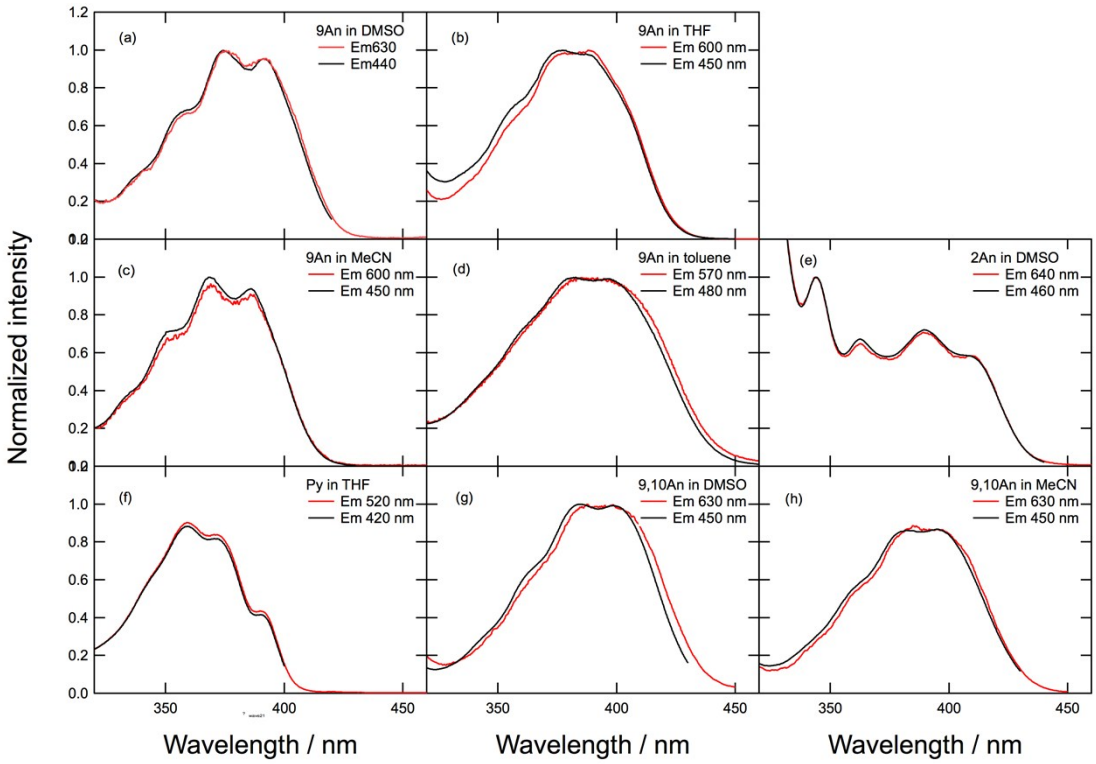

Fig. S17. Excitation spectra of (a) **9An** in DMSO, (b) **9An** in THF, (c) **9An** in THF, (d) **9An** in toluene, (e) **2An** in DMSO, (f) **Py** in THF, (g) **9,10An** in DMSO and (h) **9,10An** in MeCN in the presence of TBAAc.

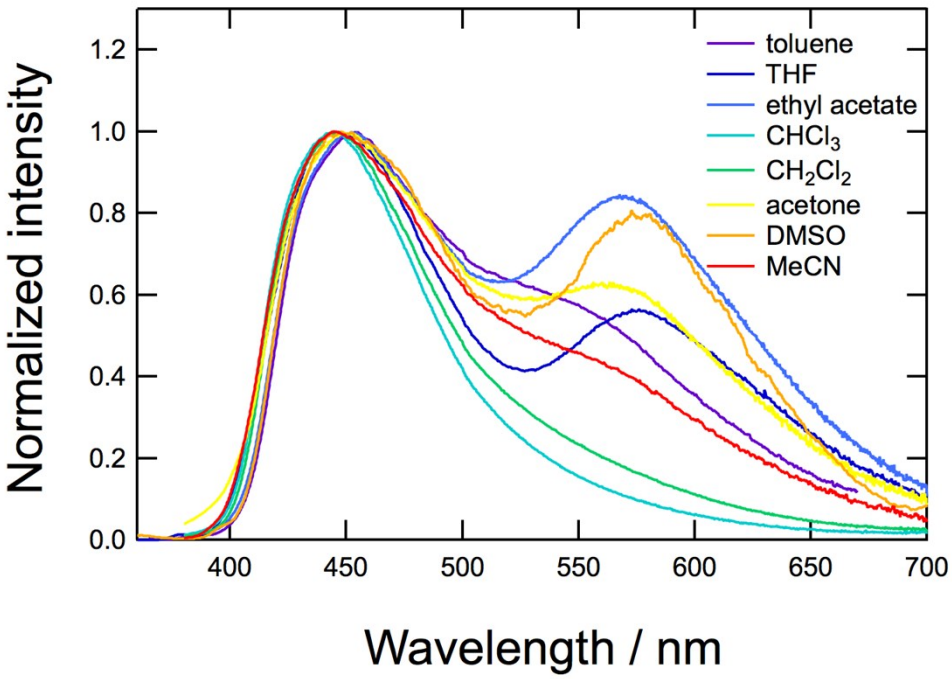

Fig. S18. Fluorescence spectra of **9An** in the toluene, THF, ethyl acetate, $CHCl_3$, CH_2Cl_2, acetone, DMSO and MeCN in the presence of TBAAc.

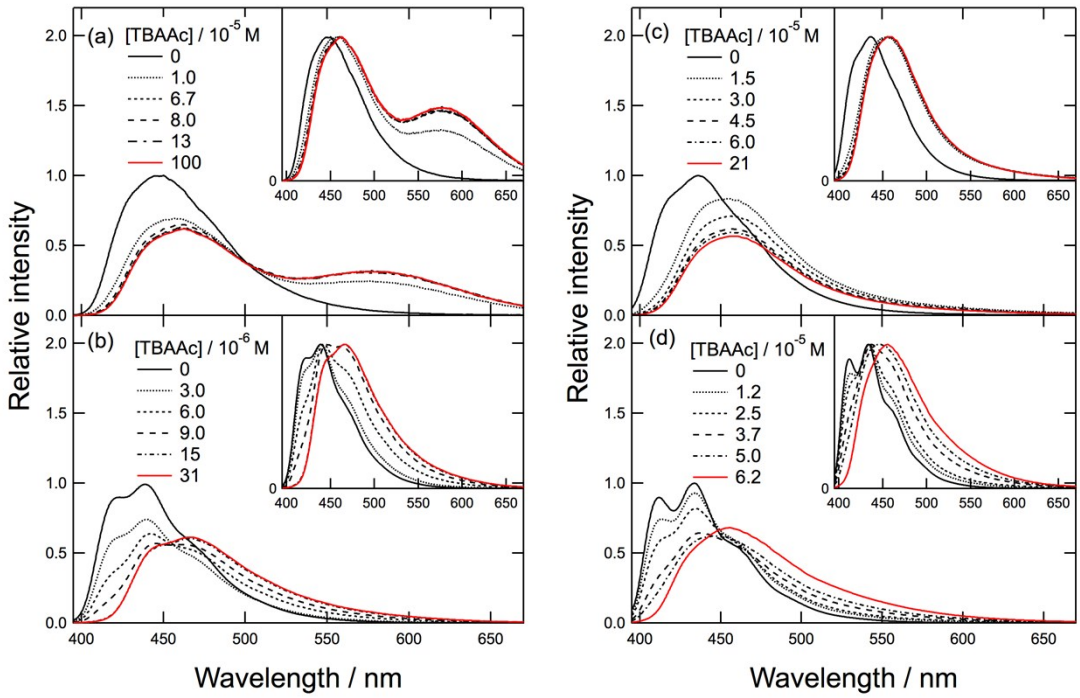

Fig. S19. Changes in the fluorescence spectra of **2An** in (a) DMSO (1.0×10^{-5} M), (b) THF (1.1×10^{-5} M), (c) MeCN (1.0×10^{-5} M) and (d) toluene (1.1×10^{-5} M) by the addition of TBAAc.

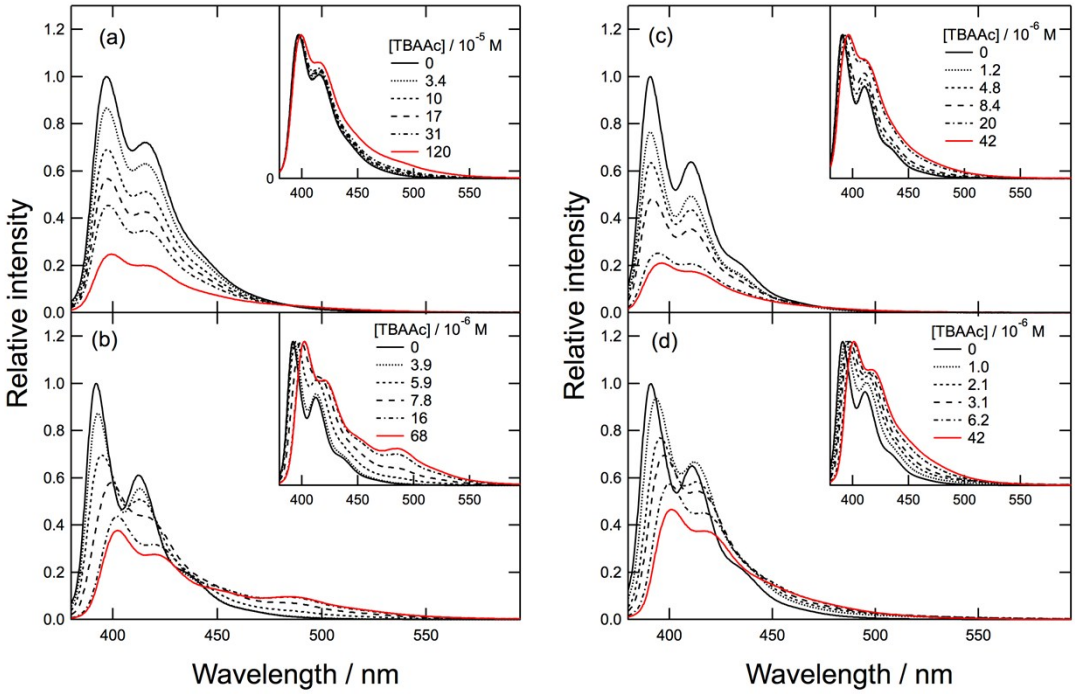

Fig. S20. Changes in the fluorescence spectra of **Py** in (a) DMSO (1.1×10^{-6} M), (b) THF (2.2×10^{-6} M), (c) MeCN (2.9×10^{-6} M) and (d) toluene (1.9×10^{-6} M) by the addition of TBAAc.

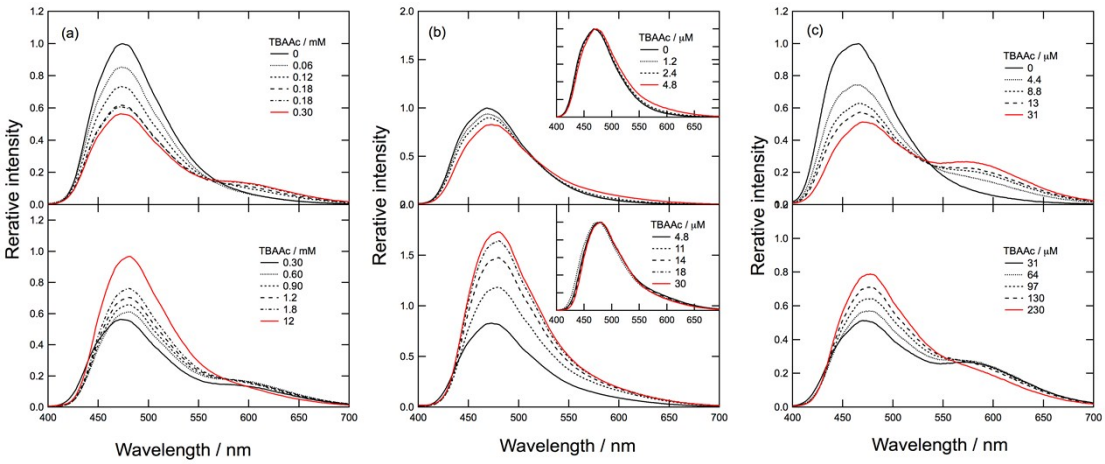

Fig. S21. Changes in the fluorescence spectra of **9,10An** in (a) DMSO (6.2×10^{-6} M), (b) THF (7.1×10^{-6} M) and (c) MeCN (7.4×10^{-6} M) by the addition of low concentration (top) and high concentration (bottom) of TBAAc.

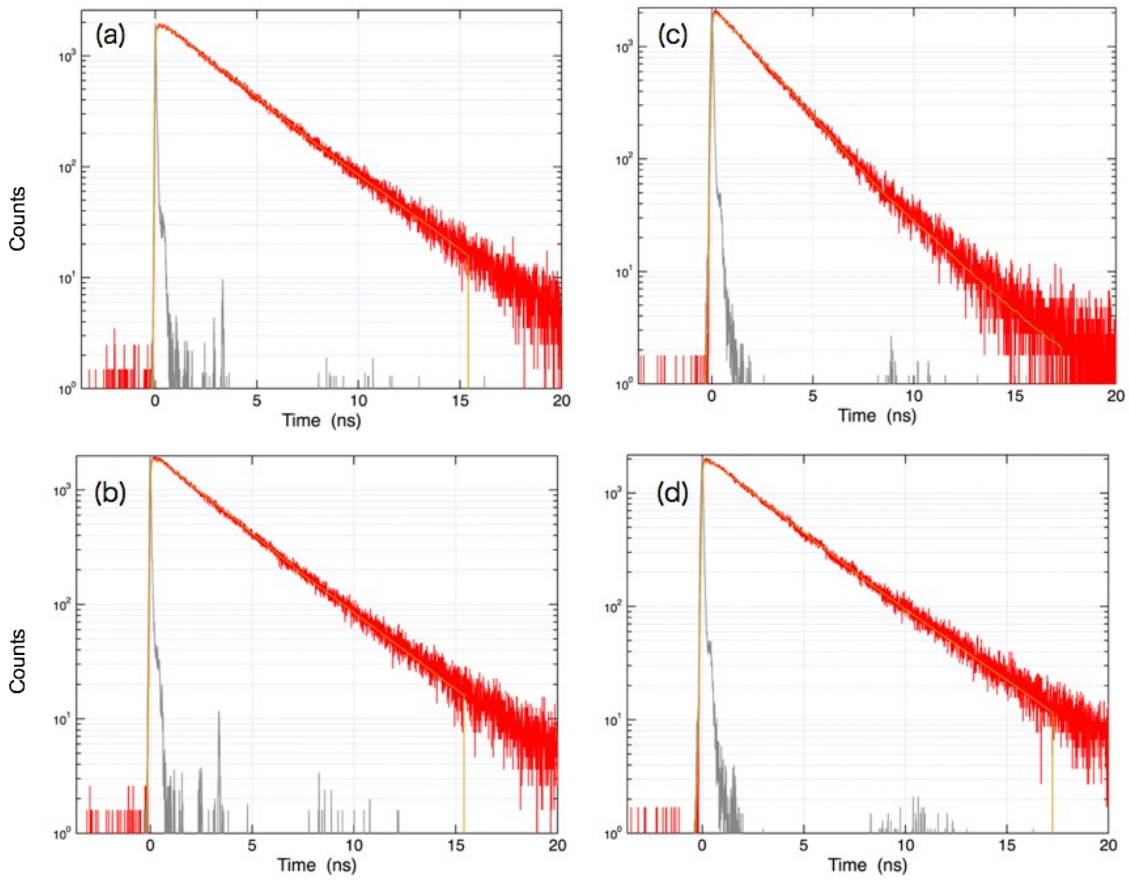

Fig. S22. Fluorescence decay of **9An** monitored at 450 nm in (a) DMSO, (b) THF, (c) MeCN and (d) toluene.

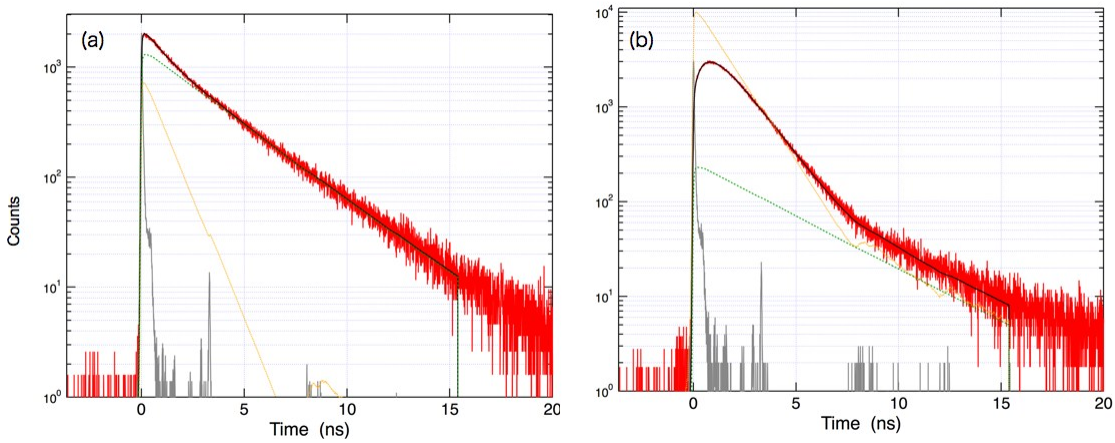

Fig. S23. Fluorescence decay of **9An** in the presence of TBAAc (3.0 mM) monitored at (a) 460 nm and (b) 640 nm in DMSO.

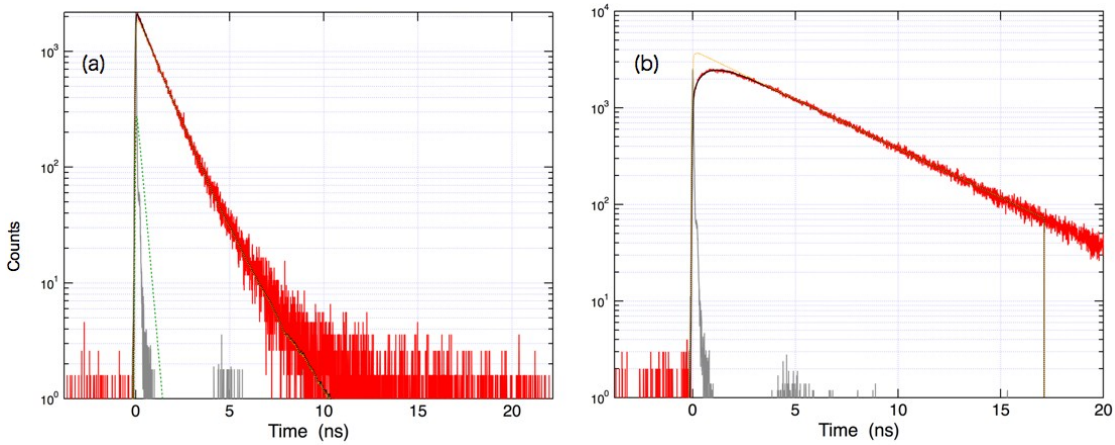

Fig. S24. Fluorescence decay of **9An** in the presence of TBAAc (0.20 mM) monitored at (a) 450 nm and (b) 650 nm in THF.

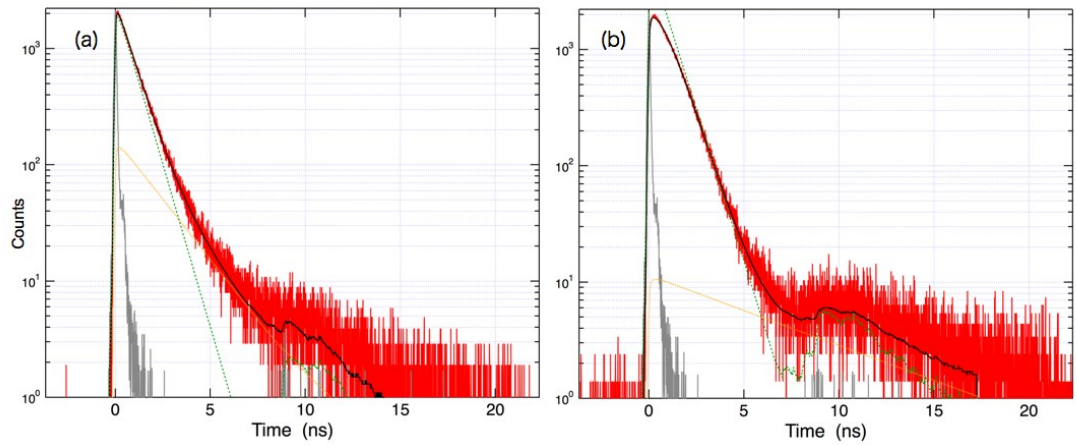

Fig. S25. Fluorescence decay of **9An** in the presence of TBAAc (0.20 mM) monitored at (a) 440 nm and (b) 630 nm in MeCN.

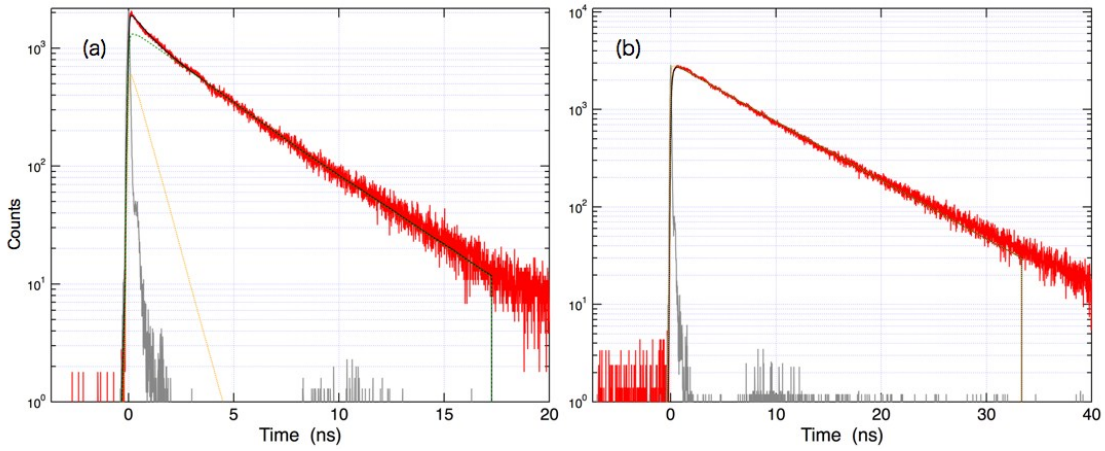

Fig. S26. Fluorescence decay of **9An** in the presence of TBAAc (0.18 mM) monitored at (a) 440 nm and (b) 630 nm in toluene.

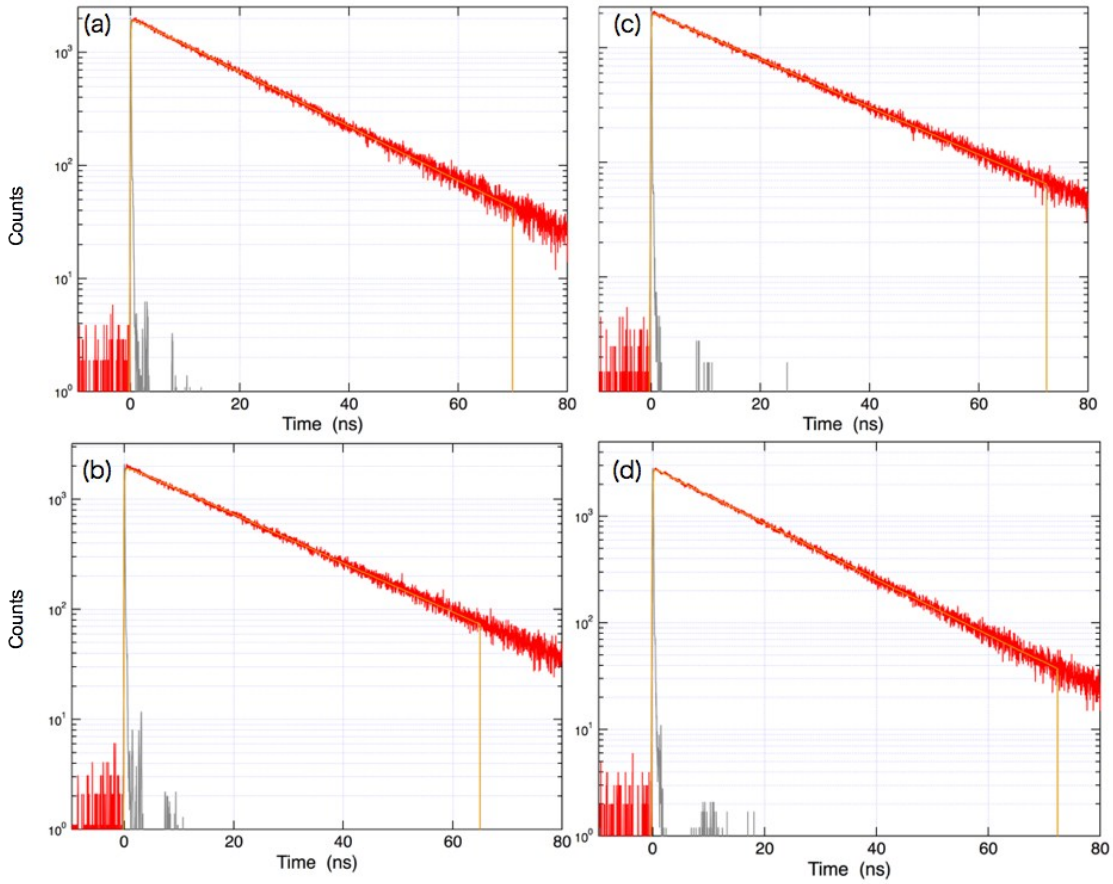

Fig. S27. Fluorescence decay of **2An** monitored at 450 nm in (a) DMSO, (b) THF, (c) MeCN and (d) toluene.

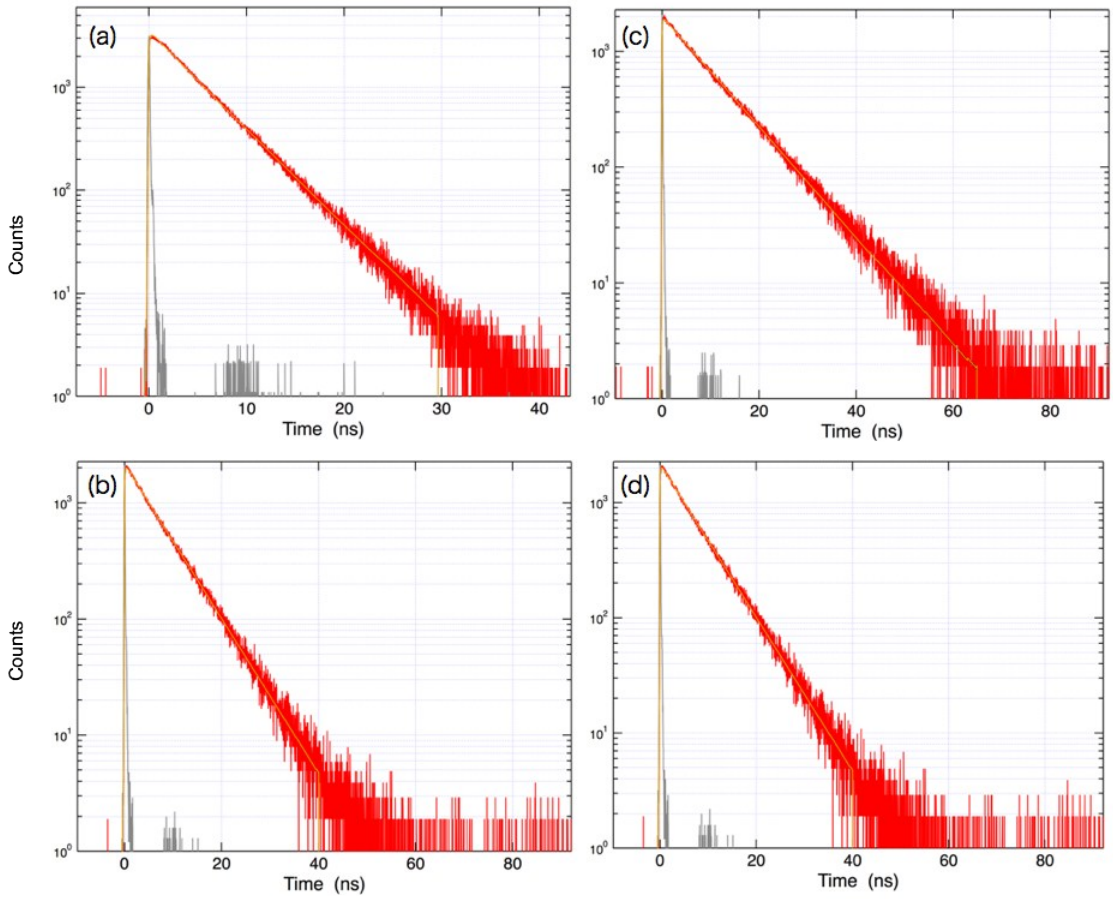

Fig. S28. Fluorescence decay of **Py** monitored at 450 nm in (a) DMSO, (b) THF, (c) MeCN and (d) toluene.

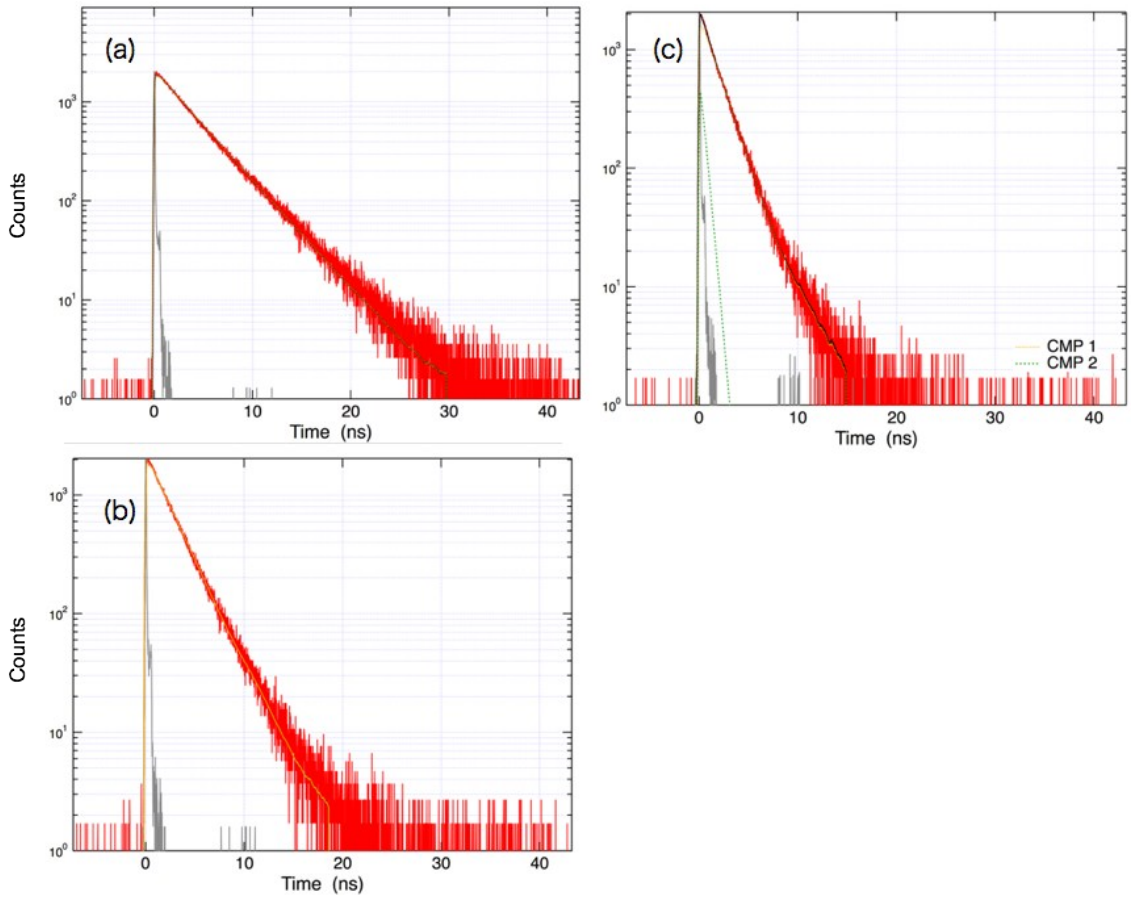

Fig. S29. Fluorescence decay of **9,10An** monitored at 450 nm in (a) DMSO, (b) THF and (c) MeCN.

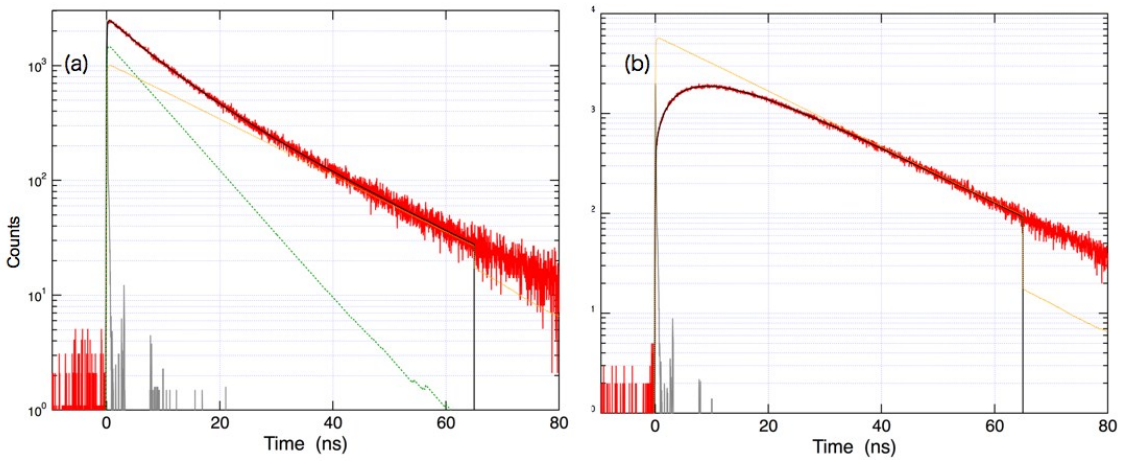

Fig. S30. Fluorescence decay of **2An** in the presence of TBAAc (1.0 mM) monitored at (a) 440 nm and (b) 630 nm in DMSO.

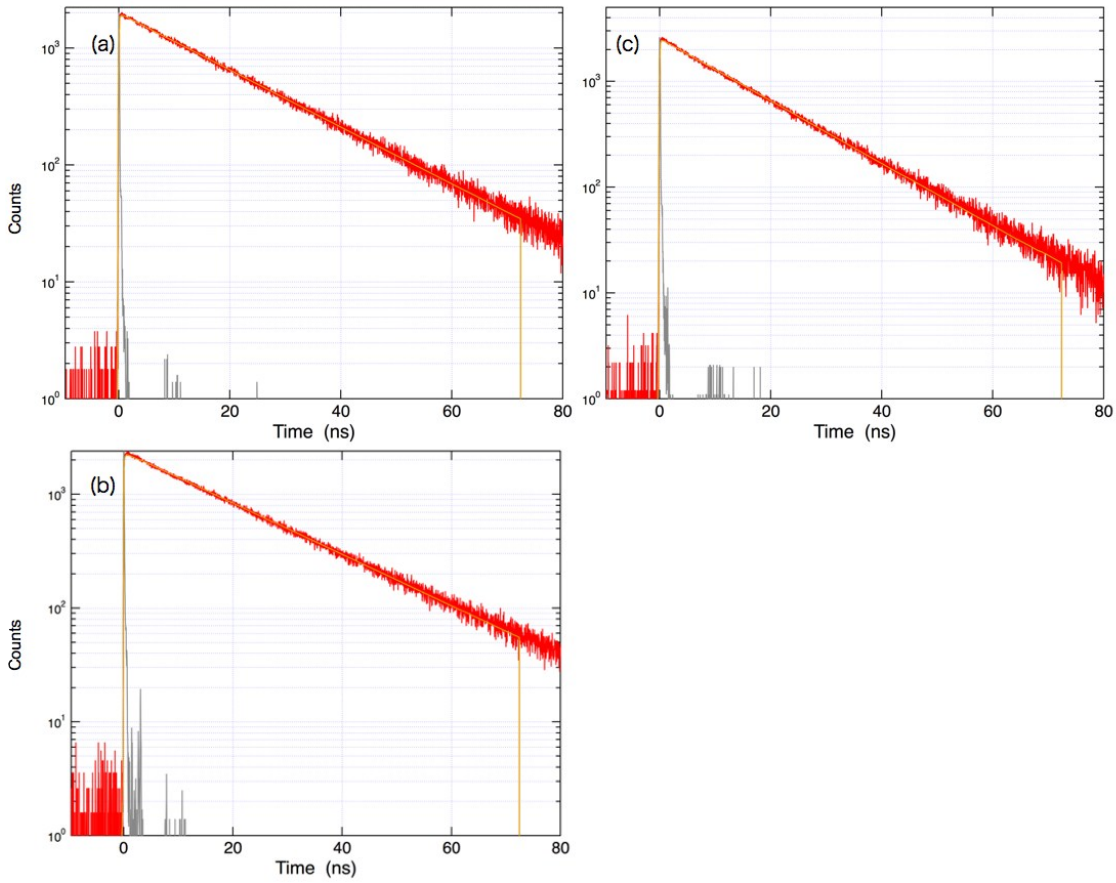

Fig. S31. Fluorescence decay of **2An** in (a) THF (0.31 mM of TBAAc), (b) MeCN (0.21 mM of TBAAc) and (c) toluene (0.062 mM of TBAAc).

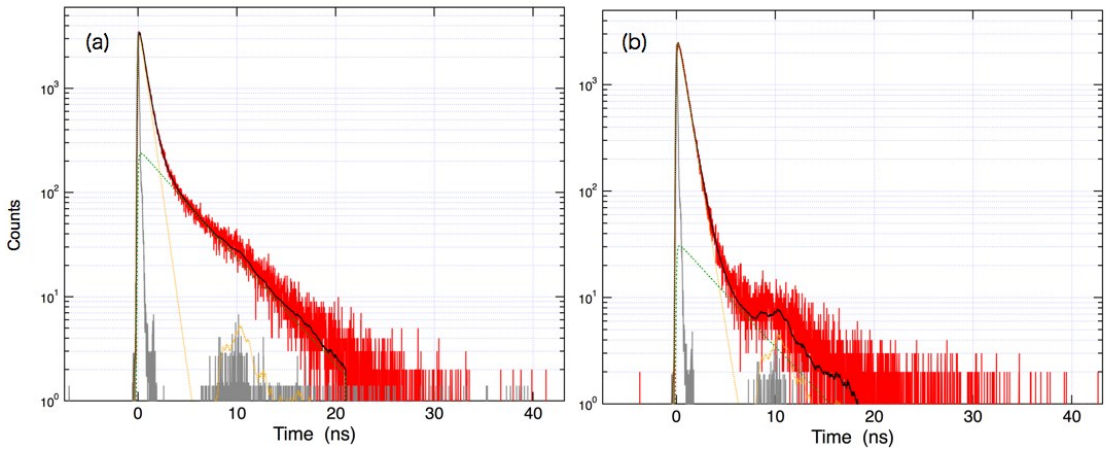

Fig. S32. Fluorescence decay of **Py** in the presence of TBAAc (1.2 mM) monitored at (a) 400 nm and (b) 530 nm in DMSO.

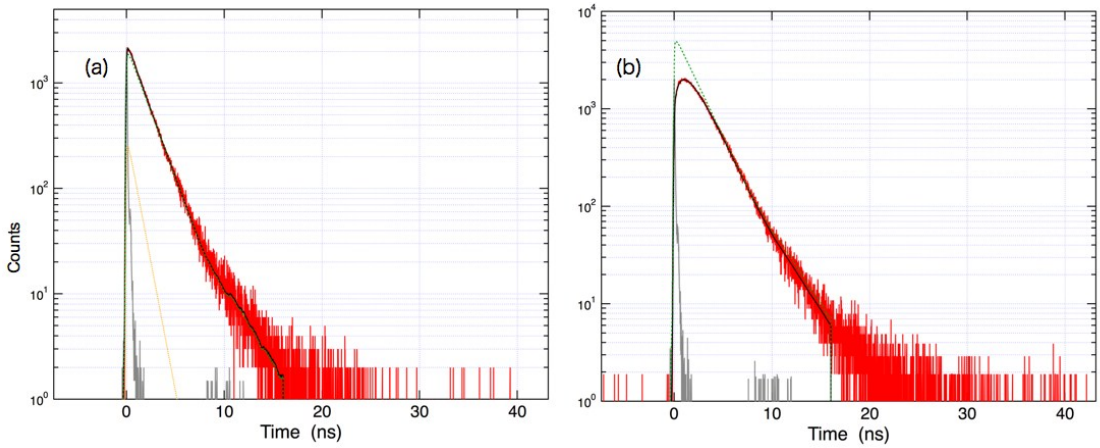

Fig. S33. Fluorescence decay of **Py** in the presence of TBAAc (6.8 mM) monitored at (a) 400 nm and (b) 530 nm in THF.

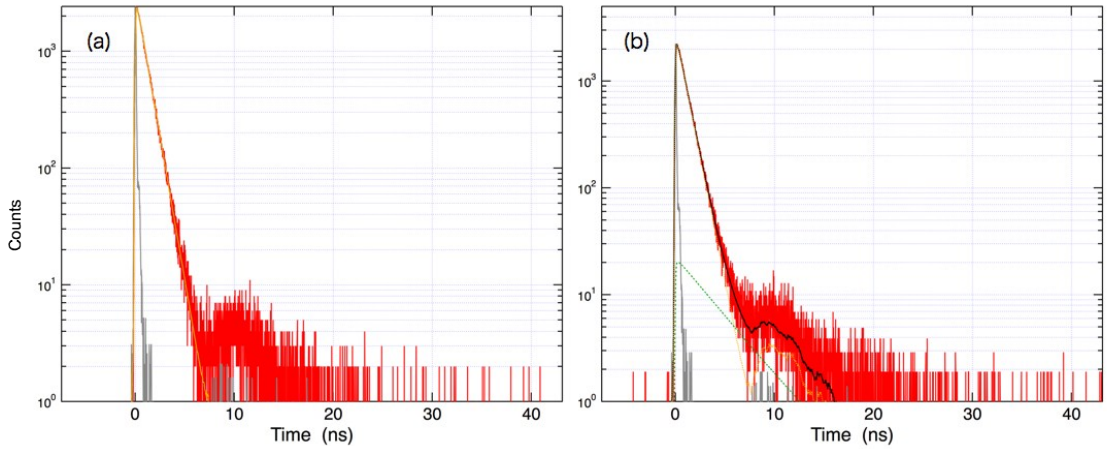

Fig. S34. Fluorescence decay of **Py** in the presence of TBAAc (0.42 mM) monitored at (a) 400 nm and (b) 530 nm in MeCN.

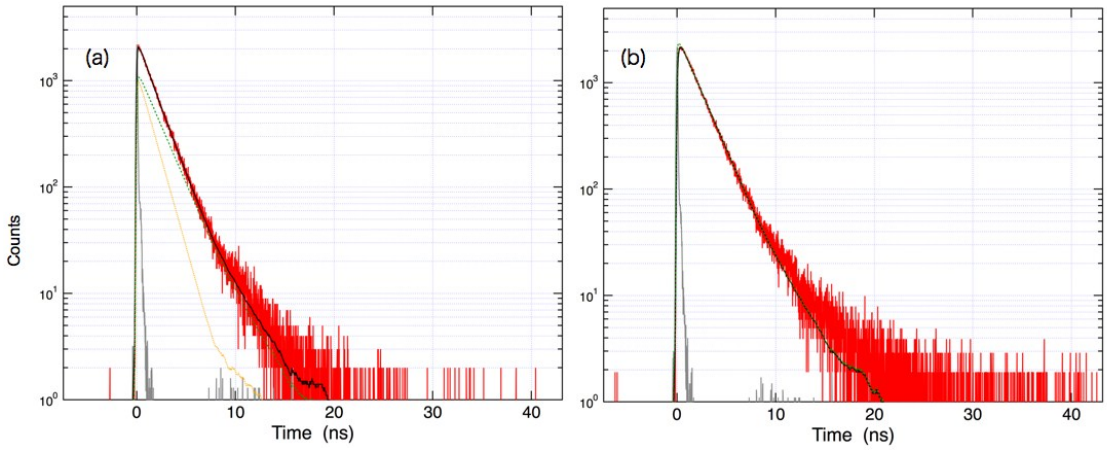

Fig. S35. Fluorescence decay of **Py** in the presence of TBAAc (0.41 mM) monitored at (a) 400 nm and (b) 530 nm in toluene.

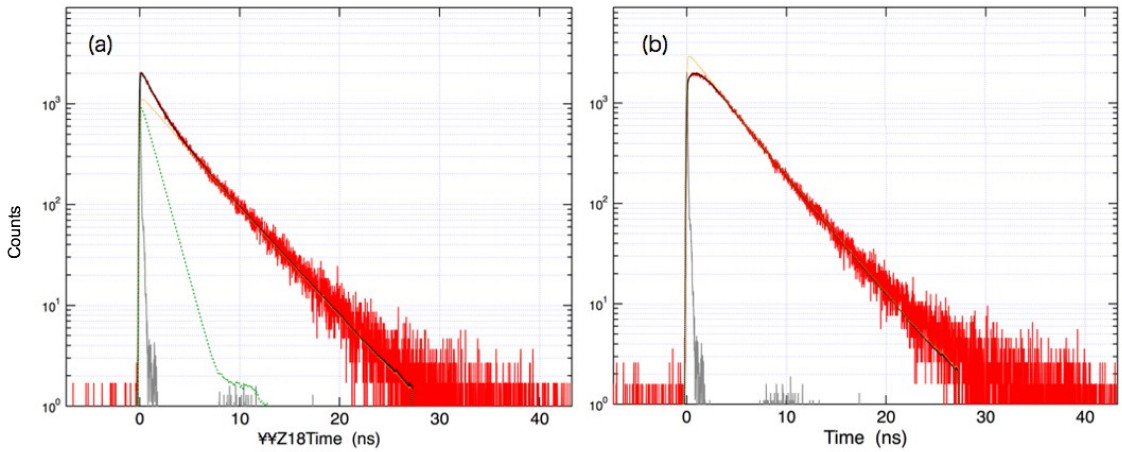

Fig. S36. Fluorescence decay of **9,10An** in the presence of TBAAc (0.30 mM) monotored at (a) 450 nm and (b) 630 nm in DMSO.

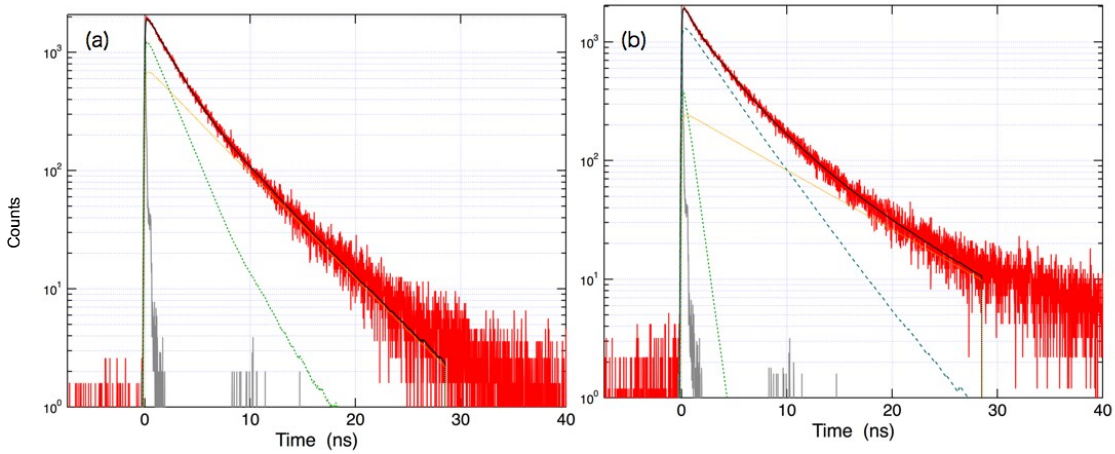

Fig. S37. Fluorescence decay of **9,10An** in the presence of TBAAc (0.048 mM) monotored at (a) 440 nm and (b) 600 nm in THF.

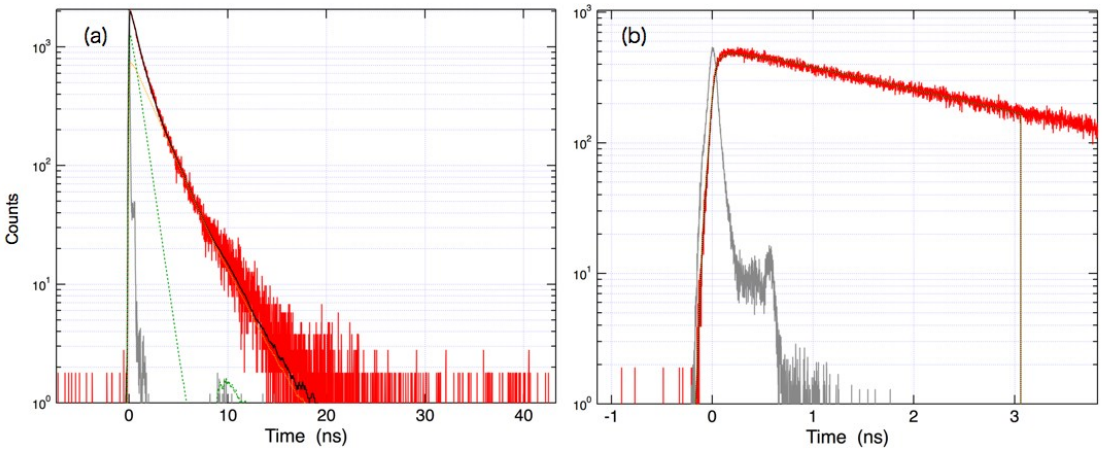

Fig. S38. Fluorescence decay of **9,10An** in the presence of TBAAc (0.031 mM) monitored at (a) 460 nm and (b) 640 nm in MeCN.

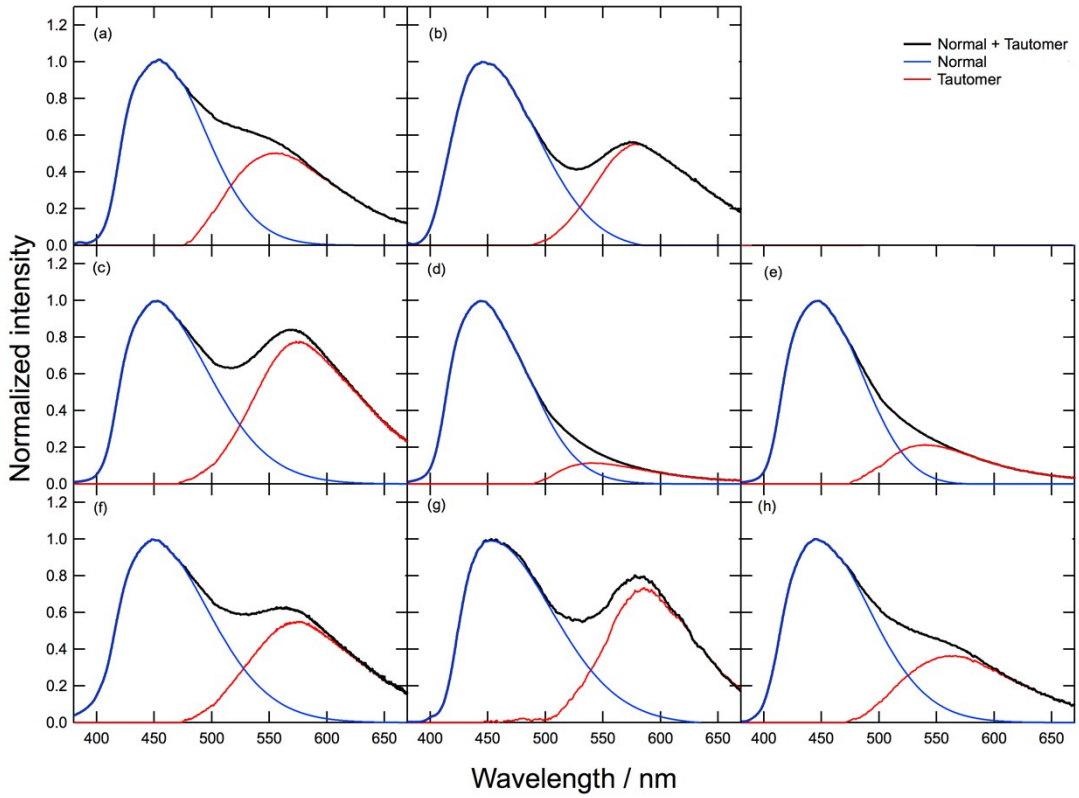

Fig. S39. Fluorescence spectra for **9An**. Normal (blue line), tautomer (red line) and normal and tautomer (black bold line) in (a) toluene, (b) THF, (c) ethyl acetate, (d) $CHCl_3$, (e) CH_2Cl_2, (f) acetone, (g) DMSO and (h) MeCN separated by subtraction.

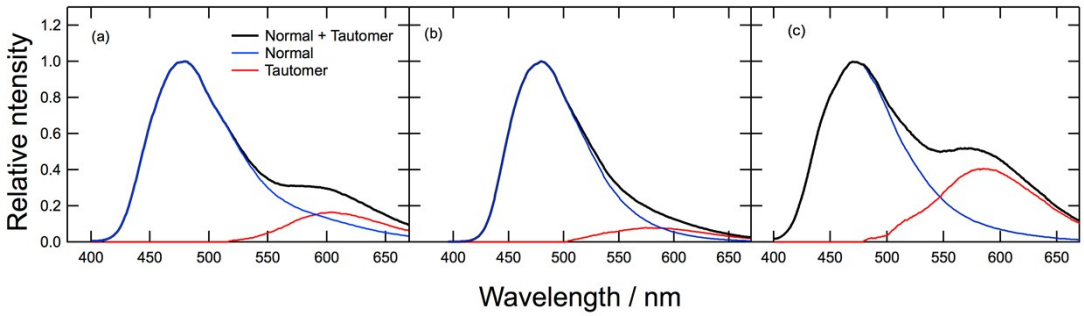

Fig. S40. Fluorescence spectra for **9,10An**. Normal (blue line), tautomer (red line) and normal and tautomer (black bold line) in (a) DMSO, (b) THF, and (c) MeCN separated by subtraction.

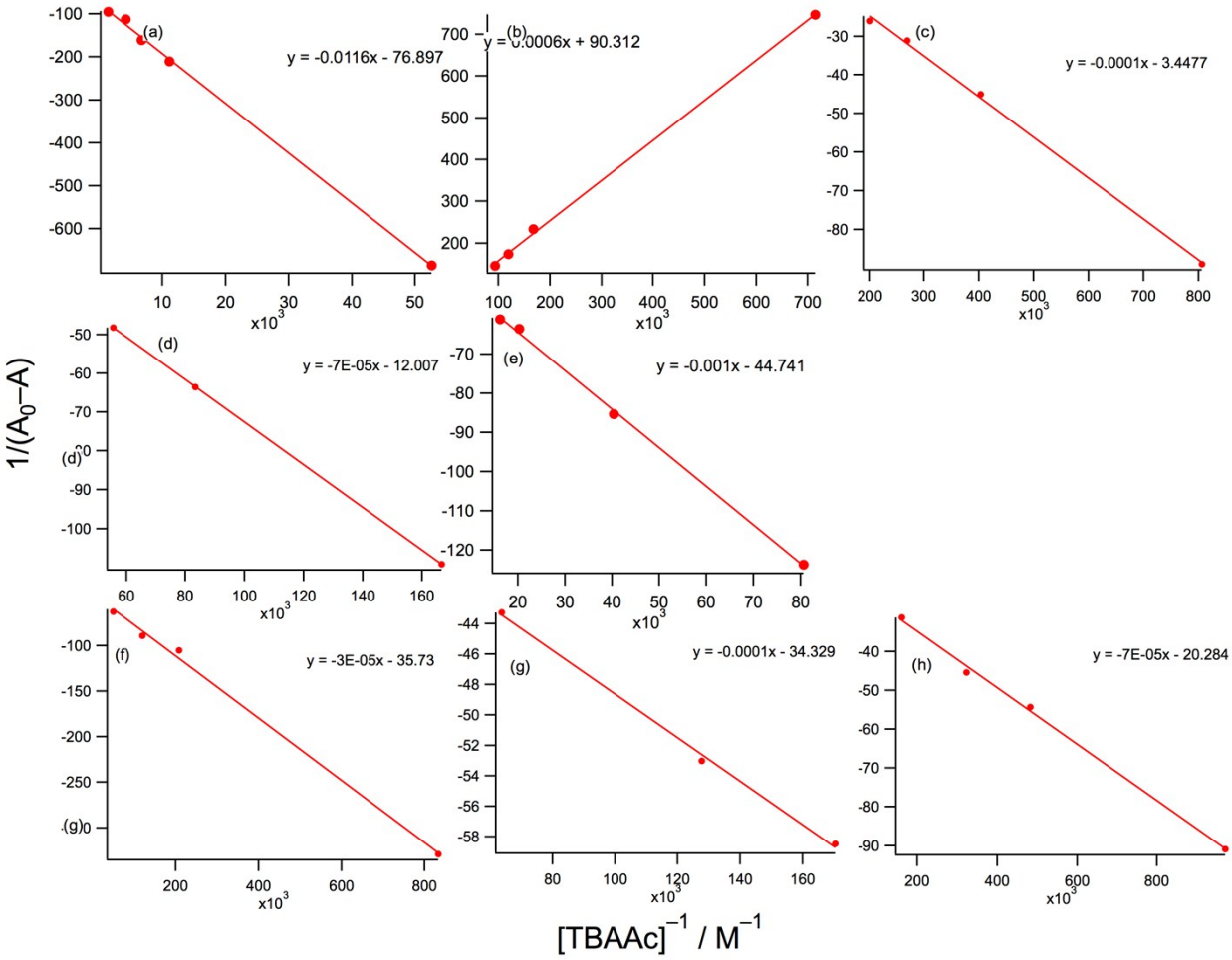

Fig. S41. Theoretical fits to estimate association constants of (a) **9An** in DMSO, (b) **9An** in THF, (c) **9An** in toluene, (d) **2An** in THF, (e) **2An** in toluene, (f) **Py** in MeCN, (g) **Py** in THF and (h) **Py** in toluene from the UV-vis titrations by the equation (a)

$$\frac{1}{A - A_0} = \frac{1}{A_{\max} - A_0}\left(\frac{1}{K_a[A]} + 1\right) \qquad \text{(a)}$$

where *A0* and *A* are the absorbances of the host in the absence and presence of TBAAc, respectively, [*A*] is the total TBAAc concentration, and A_{max} is the absorbance of host under full association with TBAAc.

Table S1. Fluorescence quantum yields (Φ_{Fl}) and lifetimes (τ) of **9An**, **2An**, **Py** and **9,10An** in DMSO, MeCN, THF and toluene

	9An				**2An**			
	DMSO	MeCN	THF	toluene	DMSO	MeCN	THF	toluene
τ [a]	2.99	2.20	3.02	3.14	17.9	20.8	19.4	16.5
Φ_{Fl}	0.20	0.16	0.18	0.24	0.78	0.65	0.59	0.67
	Py				**9,10An**			
	DMSO	MeCN	THF	toluene	DMSO	MeCN	THF	
τ [a]	4.48	8.98	6.41	13.0 (0.34) [b] 5.12 (0.66) [b]	3.81	1.78	2.40	
Φ_{Fl}	0.62	0.53	0.64	0.49	0.28	0.11	0.17	

[a] ns, [b] Normalized amplitudes

Table S2. Lifetimes of **9An**, **2An**, **Py** and **9,10An** in the presence of TBAAc in various solvents

	DMSO				MeCN				THF				toluene			
	τ [a]	Amp[b]	τ [a]	Amp[b]	τ [a]	Amp[b]	τ [a]	Amp[b]	τ [a]	Amp[b]	τ [a]	Amp[b]	τ [a]	Amp[b]	τ [a]	Amp[b]
λ / nm	460		640		440		630		450		650		440		630	
	3.07	0.62	0.73	-1.00	2.09	0.06	0.51	-1.00	1.14	0.84	0.75	-1.00	0.66	0.35	0.14	-1.00
9An	0.92	0.38	1.28	0.98	0.77	0.94	0.83	0.99	0.23	0.16	4.22	1.00	3.42	0.65	7.09	1.00
			3.78	0.02			7.13	0.01								
λ / nm	440		630		460				440				450			
	17.5	0.40	6.80	-1.00	17.7	1.00			19.2	1.00			14.6	1.00		
2An	7.67	0.60	15.2	1.00												
λ/ nm	400		530		400		530		400		530		400		530	
	4.06	0.06	4.30	0.01	8.81	1.00	3.94	0.01	1.74	0.87	0.91	-1.00	1.31	0.49	2.03	1.00
Py	0.64	0.94	0.76	0.99			0.93	0.99	0.88	0.13	2.07	1.00	2.02	0.51		
λ / nm	450		630		460		640		440		600					
	3.82	0.52	0.89	-1.00	2.32	0.34	2.48	-1.00	2.03	0.34	8.36	0.11				
9,10An	1.20	0.48	3.44	1.00	0.77	0.66	0.28	1.00	4.71	0.66	0.67	0.23				
											3.34	0.66				

[a] ns, [b]Normalized amplitude

Kinetic Analysis of Excited-state Intermolecular Proton-transfer Reaction

From the above discussion of the kinetics of the tautomer, we propose kinetics involving tautomer formation and deactivation as shown in Scheme 2. The rate constant k_{N^*} indicates the deactivation rate constant of N* including radiative and nonradiative processes. The formation rate constant of T* is k_{PT} and its reverse proton transfer process is k_{-PT}. The deactivation process of T* to the ground state is k_{T^*}, which includes radiative and nonradiative processes, as in k_{N^*}. The differential rate equations for change of concentrations of complex referred to as urea...AcO^- and tautomeric form in the excited state can be expressed as follows: [6-13]

$$\frac{d[N^*]}{dt} = -(k_{N^*} + k_{PT}) \times [N^*] + k_{-PT} \times [T^*] \quad (1)$$

$$\frac{d[T^*]}{dt} = -(k_{T^*} + k_{-PT}) \times [T^*] + k_{PT} \times [N^*] \quad (2)$$

The integration of equation (1) and (2) with given initial conditions at $t = 0$, $[N^*] = [N^*]_0$ and $[T^*] = [T^*]_0 = 0$ gives equations (3) and (4) for $[N^*]$ and $[T^*]$:

$$[N^*] = \frac{[N^*]_0}{\gamma_1 - \gamma_2} \times [(X-\gamma_2)exp(-\gamma_1 t) - (X-\gamma_1)exp(-\gamma_2 t)] \quad (3)$$

$$[T^*] = \frac{k_{PT}[N^*]_0}{\gamma_1 - \gamma_2} \times [exp(-\gamma_2 t) - exp(-\gamma_1 t)] \quad (4)$$

where

$$\gamma_1 = \frac{1}{2}\left[(X+Y) + \sqrt{(X-Y)^2 + 4k_{PT}k_{-PT}}\right] \quad (5)$$

$$\gamma_2 = \frac{1}{2}\left[(X+Y) - \sqrt{(X-Y)^2 + 4k_{PT}k_{-PT}}\right] \quad (6)$$

$$X = k_{N^*} + k_{PT}, \qquad Y = k_{T^*} + k_{-PT} \quad (7)$$

$$\gamma_1 + \gamma_2 = X + Y = k_{N^*} + k_{T^*} + k_{PT} + k_{-PT} \quad (8)$$

An iterative fitting method was applied to the deconvoluted decay curve to determine the four unknown rate constants, which are correlated with eq. 8, in the presence of TBAAc, according to a previously reported calculation method.[14] The Gibbs free energy change, ΔG^*, which is singlet energy gap between normal and tautomer form and equilibrium constant (K_{eq}) for the normal and the tautomer in the excited state at 298K were estimated as follows:[15,16]

$$\Delta G^* = -RTlnK_{eq}, \qquad K_{eq} = \frac{k_{PT}}{k_{-PT}} \quad (9)$$

These results of kinetic analysis are shown in table 3 and S3.

Table S3. Determined rate constants (s^{-1}) of **2An**, **Py** and **9,10An** in the presence of TBAAc

	2An	**Py**	**9,10An**	
Rate constants	DMSO	THF	DMSO	MeCN
k_a (s^{-1})	9.99×10^7	1.36×10^8	2.36×10^8	5.90×10^8
k_b (s^{-1})	1.07×10^8	1.00×10^9	2.91×10^8	3.19×10^8
k_{PT} (s^{-1})	2.59×10^7	5.23×10^8	2.99×10^8	4.13×10^8
k_{-PT} (s^{-1})	1.60×10^7	6.37×10^7	2.60×10^8	4.12×10^8
K_{PT}	1.43	8.20	1.11	1.01
ΔG^* (kJ/mol^{-1})	-1.20	-5.21	-0.26	–0.01

Table S4. Association constants of **9An**, **2An** and **Py** in DMSO, MeCN, THF and toluene from the UV-Vis titrations.

	DMSO	MeCN	THF	toluene
9An	6.63	–	156	34.5
2An	–	–	172	44.7
Py	–	111	240	279

K_a / 10^3 M^{-1}

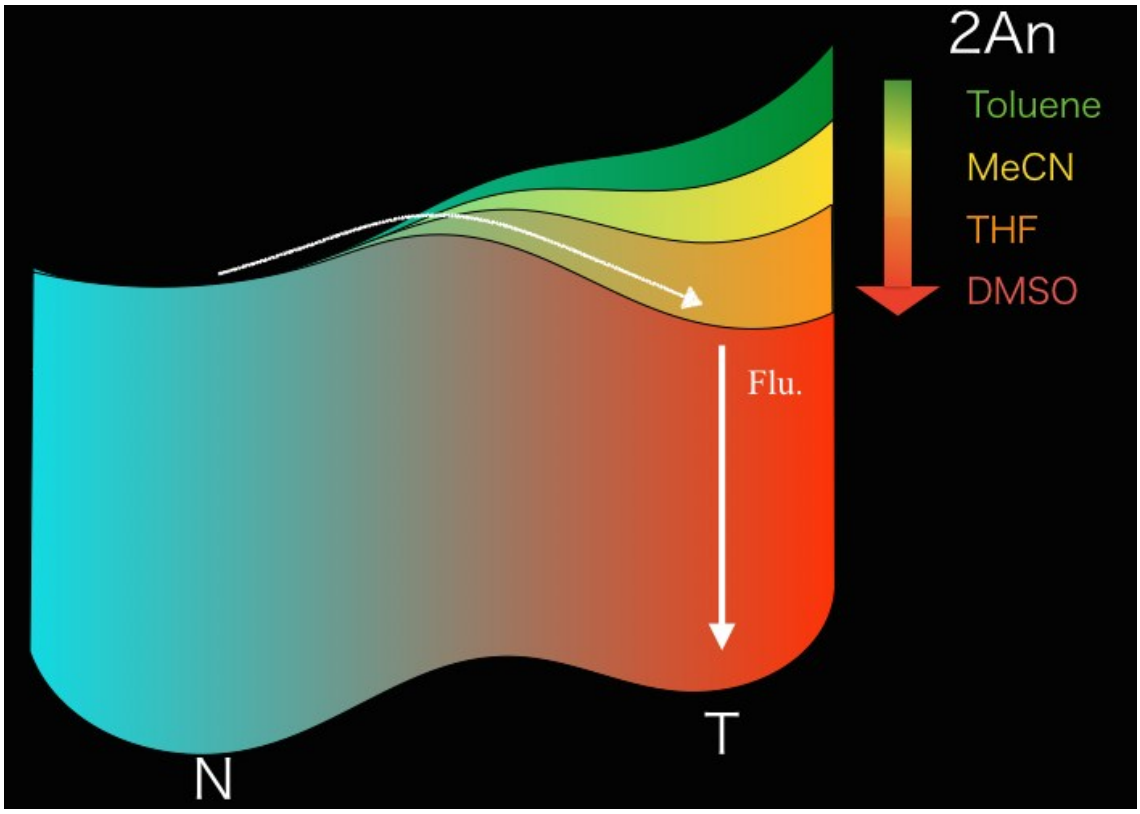

Scheme S2. Reaction scheme of ESIPT for **2An** in the presence of TBAAc.

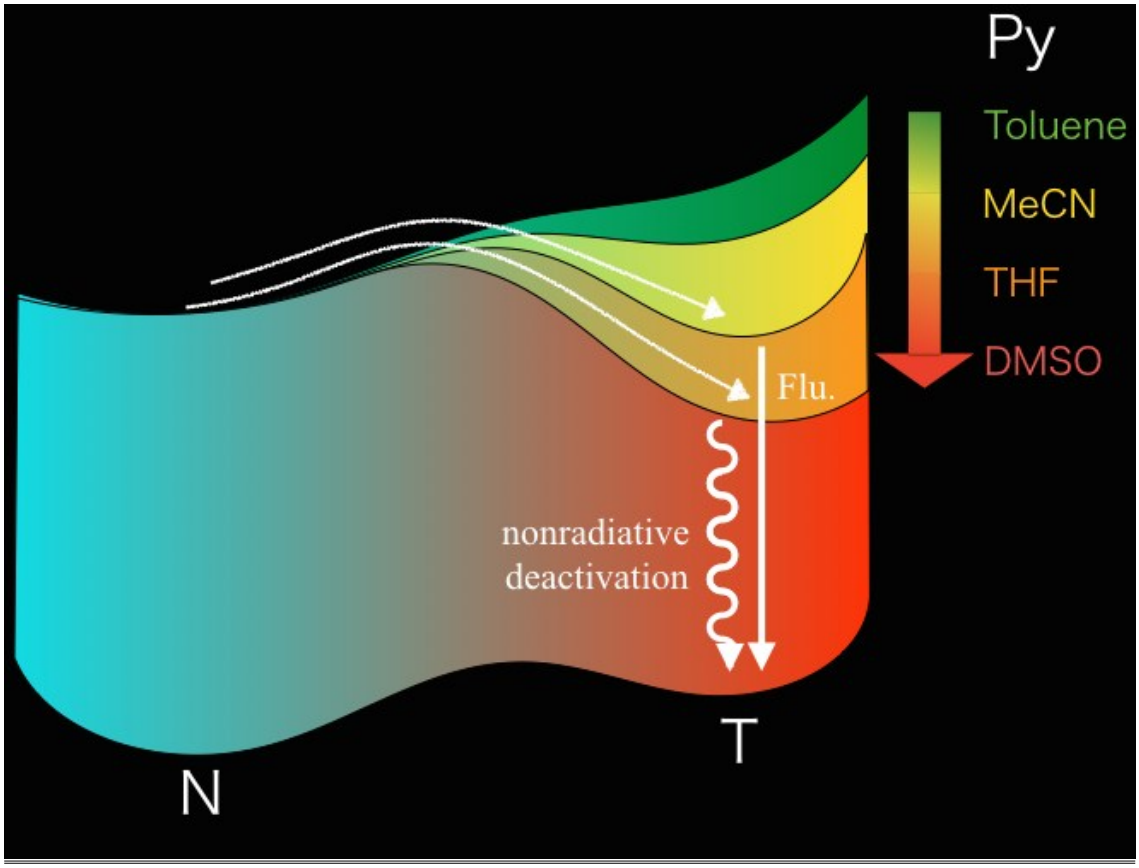

Scheme S3. Reaction scheme of ESIPT for **Py** in the presence of TBAAc.

References

1 Y. Nishimura, M. Kamada, M. Ikegami, R. Nagahata and T. Arai, The relaxation dynamics of the excited state of stilbene dendrimers substituted with phenylacetylene groups. *J. Photochem. Photobiol. A-Chem.,* 2006, **178**, 150.

2 N. Boens, N. Tamai, I. Yamazaki and T. Yamazaki, Picosecond Single Photon Timing Measurements with a Proximity Type Microchannel Plate Photomultiplier and Global Analysis with Reference Convolution. *Photochem. Photobiol.,* 1990, **52**, 911.

3 K. Ninomiya, T. Shioiri and S. Yamada, Phosphorus in Organic Synthesis.7. Diphenyl Phosphorazidate (DPPA) - New Convenient Reagent for a Modified Curtius Reaction. *Tetrahedron,* 1974, **30**, 2151.

4 L. Pescatori, A. Arduini, A. Pochini, F. Ugozzoli and A. Secchi, Design, synthesis and recognition properties of urea-type anion receptors in low polar media. *Eur. J. Org. Chem.,* 2008, **2008**, 109.

5 H. Matsumoto, Y. Nishimura and T. Arai, Fluorescence Sensor with A New ON^1–OFF–ON^2 Switching Mechanism Using the Excited State Intermolecular Proton Transfer Reaction of An Anthracene-diurea Compound. *Photochem. Photobiol.,* 2017, **93**, 1187–1192.

6 T. Okada, T. Saito, N. Mataga, Y. Sakata and S. Misumi, Solvent Effects upon Dynamic Behavior of Intramolecular Heteroexcimers. *Bull. Chem. Soc. Jpn.,* 1977, **50**, 331.

7 M. Migita, T. Okada, N. Mataga, Y. Sakata, S. Misumi, N. Nakashima and K. Yoshihara, Picosecond Laser Spectroscopy of Intramolecular Heteroexcimer Systems - Time-Resolved Fluorescence Studies of *p*-$(CH_3)_2NC_6H_4$-$(CH_2)_n$-(9-Anthryl), *p*-$(CH_3)_2NC_6H_4$-$(CH_2)_n$-(1-Pyrenyl) Systems and 9,9'-Bianthryl. *Bull. Chem. Soc. Jpn.,* 1981, **54**, 3304.

8 T. Okada, M. Migita, N. Mataga, Y. Sakata and S. Misumi, Picosecond Laser Spectroscopy of Intramolecular Heteroexcimer Systems - Time-Resolved Absorption Studies of *p*-$(CH_3)_2NC_6H_4(CH_2)_n$(1-Pyrenyl) and *p*-$(CH_3)_2NC_6H_4(CH_2)_n$-(9-Anthryl) Systems. *J. Am. Chem. Soc.,* 1981, **103**, 4715.

9 V. V. Shynkar, Y. Mely, G. Duportail, E. Piemont, A. S. Klymchenko and A. P. Demchenko, Picosecond time-resolved fluorescence studies are consistent with reversible excited-state intramolecular proton transfer in 4'-(dialkylaminoe)-3-hydroxyflavones. *J. Phys. Chem. A,* 2003, **107**, 9522.

10 Demas, J. N. *Excited State Lifetime Measurements*; Academic Press: New York, 1983; pp 59-62.

11 P. T. Chou, W. S. Yu, Y. M. Cheng, S. C. Pu, Y. C. Yu, Y. C. Lin, C. H. Huang and C. T. Chen, Solvent-polarity tuning excited-state charge coupled proton-transfer reaction in *p*-*N*,*N*-

ditolylaminosalicylaldehydes. *J. Phys. Chem. A,* 2004, **108**, 6487.

12 S. Ikedu, Y. Nishimura and T. Arai, Kinetics of Hydrogen Bonding between Anthracene Urea Derivatives and Anions in the Excited State. *J. Phys. Chem. A,* 2011, **115**, 8227.

13 S. Tasaki, A. Momotake, Y. Kanna, T. Sato, Y. Nishimura and T. Arai, Producing a dual-fluorescent molecule by tuning the energetics of excited-state intramolecular proton transfer. *Photochem. Photobiol. Sci.,* 2015, **14**, 1864.

14 Y. Nishimura, K. Shimamura, Y. Ohmori, Y. Shinohara and T. Arai, Kinetic studies of emissive guanine derivatives bearing anthracene moiety. *J. Photochem. Photobiol. A-Chem.,* 2011, **218**, 69.

15 K. C. Tang, M. J. Chang, T. Y. Lin, H. A. Pan, T. C. Fang, K. Y. Chen, W. Y. Hung, Y. H. Hsu and P. T. Chou, Fine Tuning the Energetics of Excited-State Intramolecular Proton Transfer (ESIPT): White Light Generation in A Single ESIPT System. *J. Am. Chem. Soc.,* 2011, **133**, 17738.

16 H. Masai, S. Ikedu, Y. Nishimura and T. Arai, Kinetic analysis of photoinduced reactions in hydrogen-bonded complexes of anthracene-urea with anions. *J. Photochem. Photobiol. A-Chem.,* 2012, **250**, 1.